Plant Physiology and Biochemistry 202 (2023) 107976

Contents lists available at ScienceDirect

Plant Physiology and Biochemistry

journal homepage: www.elsevier.com/locate/plaphy

Selenate triggers diverse oxidative responses in *Astragalus* species with diverse selenium tolerance and hyperaccumulation capacity

Réka Szőllősi [a], Árpád Molnár [a], Patrick Janovszky [b], Albert Kéri [b], Gábor Galbács [b], Mihály Dernovics [c], Zsuzsanna Kolbert [a,*]

[a] Department of Plant Biology, University of Szeged, Közép alley 52, 6726, Szeged, Hungary
[b] Department of Inorganic and Analytical Chemistry, University of Szeged, Dóm square 7, 6720, Szeged, Hungary
[c] Department of Plant Physiology, Agricultural Institute, Centre for Agricultural Research, Eötvös Loránd Research Network, Brunszvik str. 2., 2462, Martonvásár, Hungary

ARTICLE INFO

Handling Editor: Dr K Kees Venema

Keywords:
Astragalus bisulcatus
Astragalus cicer
Hyperaccumulation
Oxidative stress
Selenate
Tolerance

ABSTRACT

Selenium (Se) hyperaccumulators are capable of uptake and tolerate high Se dosages. Excess Se-induced oxidative responses were compared in *Astragalus bisulcatus* and *Astragalus cicer*. Plants were grown on media supplemented with 0, 25 or 75 μM selenate for 14 days. Both *A. bisulcatus* and *A. cicer* accumulated >2000 μg/g dry weight Se to the shoot but the translocation factors of *A. cicer* were below 1 suggesting its non hyperaccumulator nature. *A. cicer* showed Se sensitivity indicated by reduced seedling fresh weight, root growth and root apical meristem viability, altered element homeostasis in the presence of Se. In Se-exposed *A. bisulcatus,* less toxic organic Se forms (mainly MetSeCys, γ-Glu-MetSeCys, and a selenosugar) dominated, while these were absent from *A. cicer* suggesting that the majority of the accumulated Se may be present as inorganic forms. The glutathione-dependent processes were more affected, while ascorbate levels were not notably influenced by Se in either species. Exogenous Se triggered more intense accumulation of malondialdehyde in the sensitive *A. cicer* compared with the tolerant *A. bisulcatus*. The extent of protein carbonylation in the roots of the 75 μM Se-exposed *A. cicer* exceeded that of *A. bisulcatus* indicating a correlation between selenate sensitivity and the degree of protein carbonylation. Overall, our results reveal connection between oxidative processes and Se sensitivity/tolerance/hyperaccumulation and contribute to the understanding of the molecular responses to excess Se.

1. Introduction

Up to now numerous studies have assessed that higher plants basically do not require selenium (Se) for their physiological processes (White, 2017; Chauhan et al., 2019; Hasanuzzaman et al., 2020; L. Yang et al., 2022). Due to its chemical similarity to sulfur (S), Se is absorbed and metabolized by higher plants *via* the routes of S assimilation (White, 2018). Regarding Se tolerance, plant species can be grouped into various categories: non-accumulators, Se-indicators and Se-(hyper)accumulators (White, 2017, 2018; Hasanuzzaman et al., 2020). Non-accumulators (or Se-sensitive plants) include *e.g. Arabidopsis thaliana* or grasses, Se-indicator species are known in Fabaceae or Asteraceae which generally grow in Se-deficient or low Se containing soils (Gupta and Gupta, 2017). Meanwhile, high Se concentration in soils does not always seem to be hazardous for plants (Gupta and Gupta, 2017; White, 2018; Pilon-Smits, 2019). Plants native to Se-rich areas have the capability not only to tolerate but also to accumulate Se. These Se-(hyper)accumulators also show taxonomic diversity, *e.g.* the most notorious Se-(hyper) accumulators are *Stanleya pinnata* from Mustard family and *Astragalus biculcatus* from Fabaceae (Freeman et al., 2006; Statwick et al., 2016; Schiavon and Pilon-Smits, 2017; Pilon-Smits, 2019). Within *Astragalus* genus both non-accumulators such as *A. cicer* (Statwick et al., 2016) or *A. membranaceus* (Kolbert et al., 2018) and Se-(hyper)accumulators like *A. bisulcatus* or *A. racemosus* (White, 2016) can be found.

However, majority of the plant species cannot tolerate elevated doses of soil Se due to the synthesis of malfunctional selenoproteins, the promotion of disturbance in hormonal and nutritional homeostasis, or the behaviour of Se as a pro-oxidant (Byrne et al., 2010; Kolbert et al., 2016; Hasanuzzaman et al., 2020; Szőllősi et al., 2022a). High Se concentrations induce the accumulation of reactive oxygen species (ROS) like superoxide ($O_2^{\bullet-}$), hydrogen peroxide (H_2O_2) and hydroxyl radical ($OH^{\bullet}$), leading to oxidative stress (Silva et al., 2018). It is known that a

* Corresponding author.
E-mail address: ordogne.kolbert.zsuzsanna@szte.hu (Z. Kolbert).

https://doi.org/10.1016/j.plaphy.2023.107976
Received 14 June 2023; Received in revised form 8 August 2023; Accepted 16 August 2023
Available online 18 August 2023

well-organized cooperation of non-enzymatic antioxidants (such as glutathione, GSH; ascorbate, AsA) and antioxidant enzymes like superoxide dismutase (SOD), catalase (CAT) and various peroxidases (PODs), is responsible for maintaining redox homeostasis within plant cells (Rajput et al., 2021). It has been proposed that the visible Se toxicity symptoms are the consequences of increased level of lipid peroxidation, glutathione depletion, chlorophyll degradation, as well as decreased activity of SOD, CAT or PODs (Hawrylak-Nowak et al., 2015; Khalofah et al., 2021; Lv et al., 2021).

Contrary, in Se-hyperaccumulator *Stanleya pinnata* higher levels of AsA, GSH and nonprotein thiols were found compared to secondary Se accumulator *Stanleya albescens* (Freeman et al., 2006). Moreover, Wang et al. (2018) revealed that glutathione-related genes and genes encoding peroxidases are differentially expressed in Se-hyperaccumulator *Stanleya pinnata* compared to the non-accumulator *S. elata* and many of them showed constitutively higher expression in *S. pinnata*. These data suggest that Se tolerance and Se hyperaccumulating ability may be in correlation with a higher antioxidant capacity (Szőllősi et al., 2022b).

It has been stated that Se toxicity is generally accompanied by nitro-oxidative stress due to the pro-oxidant nature of excess Se (Van Hoewyk, 2013; Chen et al., 2014; Kolbert et al., 2016, 2019a). In our previous study (Kolbert et al., 2018), it was found that in Se hyperaccumulator *Astragalus bisulcatus* excess Se does not provoke substantial ROS/reactive nitrogen species (RNS) accumulation while in non-tolerant *Astragalus membranaceus* Se sensitivity was due to the Se-induced disturbance of superoxide metabolism and overproduction or imbalanced metabolism of RNS (nitric oxide, peroxynitrite and *S*-nitrosoglutathione). However, our knowledge is still insufficient about the relationship between the capability of tolerating high Se levels and the capability of controlling oxidative processes in higher plants. We hypothesize that beyond ROS and/or RNS overproduction other molecular mechanisms are involved in the Se-tolerance or intolerance of plants.

Therefore, this comparative study aims to unfold the possible differences in Se-modified ROS production and scavanging using *A. bisulcatus* as a Se hyperaccumulator and *A. cicer* which is considered to be a non-accumulator of Se (Statwick et al., 2016). Also, the oxidative modifications of proteins triggered by Se has been examined. Furthermore, we aimed to find any connection between Se tolerance/toxicity and endogenous hydrogen sulfide (H_2S) level, since it has been shown to be involved in Se-induced stress responses of plants (Chen et al., 2014; Corpas et al., 2019; Szőllősi et al., 2021).

2. Materials and methods

2.1. Plant material and growing conditions

Astragalus bisulcatus (Hook.) A. Gray seeds were purchased from B&T World Seeds (Aigues-Vives, France), and *Astragalus cicer* (L.) seeds were kindly provided by the Botanical Garden of University of Szeged (Szeged, Hungary). The seeds were surface sterilized with 20% (v/v) sodium hypochlorite for 20 min, and washed with sterile distilled water four times in 20 min, according to the method described in our previous paper (Kolbert et al., 2018). After drying we scarified the seeds one by one using P-400 sanding paper in order to taper the external seed coat and facilitate the germination process. Seeds were placed on agar medium (the scratched surface of the seeds contacted the medium). Plastic, square Petri dishes contained half-strength Murashige and Skoog medium [0.8% (v/v) agar, 1% sucrose] supplemented with 0 (control), 25 or 75 μM sodium selenate ($Na_2SeO_4{\cdot}10\ H_2O$, VWR) based on a pilot experiment. Both plant species were grown under controlled conditions (150 μmol/m^2/s photon flux density,12 h/12 h light/dark cycle, relative humidity 55–60% and temperature, 25 ± 2 °C) for 14 days.

2.2. Evaluation of germination, growth parameters, root cell viability

Germinated seeds were counted in each Petri dish and germination percentage (%, GP) was calculated according to the following formula: number of seeds germinated/total number of seeds x 100. Fresh weight (FW) of the 14-day-old seedlings were measured using a balance, and the values are given in milligrams. Dry weight (DW) of the plantlets was recorded after a 7-day-long drying period at room temperature, and the values are given in milligrams. Primary root (PR) lengths were measured manually using a ruler and are expressed in centimeter. Cell viability of the root apical meristem (RAM) was determined by using fluorescein diacetate (FDA) fluorophore according to Lehotai et al. (2011). Root tips were incubated in 10 μM FDA solution (prepared in 10/50 mM MES/KCl buffer, pH 6.15) for 30 min in darkness and were washed four times in buffer. Data were acquired from three separate generations.

2.3. Evaluation of Se content by ICP-MS

For the measurement of Se content of both *Astragalus* species, we harvested cotyledons and roots separately, rinsed them with distilled water and dried them at room temperature for 7 days. The samples were acid digested in a microwave sample preparation device (MarsXpress CEM) at 200 °C and 1600 W for 15 min in a mixture of nitric acid [65% (w/v)] and H_2O_2 [30% (w/v), Kolbert et al., 2018]. After appropriate dilutions with distilled water, the samples were transferred to 20 mL Packard glasses. Se concentrations were determined on an Agilent 7700x inductively coupled plasma mass spectrometer (ICP-MS). The instrument was used in the helium mode of the OSR^3 collisional cell. Prior to all measurements, the autotuning of the ICP-MS instrument was performed according to manufacturer specifications, using standard tuding solutions supplied by Agilent. Sample introduction was performed by the IAS system, with an uptake rate of 600 μL/min. ICP plasma and interface parameters were set up according to standard conditions (RF forward power: 1550 W, plasma gas flow rate: 15.0 L/min, carrier gas flow rate: 1.05 L/min, sampling depth: 10.0 mm). Calibrating solutions were prepared from an ICP-MS certified monoelemental Se stock standard solution (Certipur, Merck), trace quality deionized lab-water (Millipore Elix Advantage 5 + Synergy) and 1 %(v/v)) nitric acid (BDH Aristar Ultra) to perform a multi-point, matrix-matched calibration. Signals at ^{77}Se and ^{82}Se were utilized for quantitation. Labware were cleaned before use with ultratrace nitric acid and hydrochloric acid (BDH Aristar Ultra), followed by a thorough rinsing with trace quality deionized lab-water and finally dried under a laminar flow clean bench. Results for the Se content are given in μg/g DW. The analysis was performed with three repetitions for each species, treatment and plant organ (n = 3). Translocation factors were calculated as follows: Se concentration in the shoot (μg/g DW)/Se concentration in the root (μg/g DW).

2.4. Selenium speciation with LC-high resolution-MS

Sample extraction was carried out according to Szalai et al. (2022). Briefly, samples in the range of 0.05–0.1 g were accurately weighed into 2.0 mL safety Eppendorf tubes, with the addition of 1.0 mL of 70% (v/v) methanol. After vortex mixing, the tubes were inserted into a pre-cooled (−18 °C) tube holder, and the extraction was carried out in a 1600 MiniG® - Automated Tissue Homogenizer and Cell Lyser (SPEX; Rickmansworth, UK) for 3 min at 1500 rpm. The samples were then centrifuged at 15,000 x g for 15 min at +4 °C, after which the supernatants were recovered and placed in separate Eppendorf tubes. The residues were re-extracted with 1.0 mL of 70% (v/v) methanol in a MiniG® instrument (3 min), followed by centrifugation as described above. The matching supernatants were pooled and 1 + 1 (v/v) diluted with water containing 0.2% (v/v) formic acid. After dilution, the sample solutions were filtered through 0.22 μm pore-sized disposable PTFE syringe filters and injected into the LC-MS set-up.

A Vion ion mobility quadrupole time-of-flight mass spectrometer (Waters Corporation; Milford, MA, USA) equipped with an UniSpray (Waters) ion spray source was applied. Chromatographic elution was

provided by an Acquity UPLC I-Class system (Waters) using a BEH-C18 reversed phase (RP) UPLC column (100 mm × 2.1 mm x 1.7 μm; Waters). The UniSpray ion source was used both in positive and negative ionisation modes either with MS^E or with MS^E-MSMS/DDA functions. The instrument was controlled using UNIFI software (version 1.9.4; Waters). The related instrumental parameters are described in Table S1. The search for organic selenium species was based on the study of Ouerdane et al. (2020).

2.5. Mapping of element distribution by LIBS

To assess the effect of Se treatment on the macro- and microelement distribution of *Astragalus* seedlings, laser-induced breakdown spectroscopy (LIBS) was applied (Limbeck et al., 2021). The plantlets were carefully removed from the Petri dishes with tweezers and their roots were rinsed with deionized water to wash the remaining of the cultivation medium. Seedlings were then pressed, dried and mounted on a glass microscope slide with double-sided foam tape.

The spectra were taken by using the J200 LA-LIBS tandem spectrometer (Applied Spectra Inc., USA) with the following settings: laser pulse energy 14 mJ, spot size 60 μm, integration time 1.05 ms, gate delay 0.5 μs, and repetition rate 10 Hz. The laser parameters were set to collect data from the whole sample surface with no overlapping measurement points, and from each location, only one spectrum was recorded with a spectral resolution of 0.07 nm, in the range of 190–1100 nm.

2.6. Evaluation of oxidative stress parameters

2.6.1. In situ detection of ROS and hidrogen sulfide in the root tips

Dihydroethidium (DHE) at 10 μM concentration was applied to determine the level of superoxide anion, according to the method detailed in Kolbert et al. (2012). Root segments were incubated at 37 °C for 30 min, in darkness, then washed twice with TRIS-HCl buffer (10 mM, pH 7.4).

Hydrogen peroxide (H_2O_2) levels were assessed using 50 μM Amplex Red (AR; 10-acetyl-3,7 dihydroxyphenoxazine) dye dissolved in sodium phosphate buffer (50 mM, pH 7.5) at room temperature for 30 min in darkness, and washed once with the same buffer as described in Lehotai et al. (2012).

To detect the levels of cellular H_2S we used Washington Stat Probe 1 (WSP-1) according to the method of Chen et al. (2014). The roots of the plantlets were incubated in 20 μM of WSP-1 solution prepared with 20 mM HEPES-NaOH (pH 7.5) buffer for 40 min at room temperature. Then the roots were washed with distilled water three times and were put on microscopic slides for fluorescence microscopic visualization.

All analyses were carried out three times with at 10–12 samples of each species and treatment (n = 10−12). All fluorescent microscopic analysis was performed using a Zeiss Axiovert 200M inverted microscope (Carl Zeiss) equipped with a digital camera (AxiocamHR, HQ CCD, Carl Zeiss). Filter set 10 (excitation, 450–490; emission, 515–565 nm) was used for FDA and WSP-1 probes, filter set 9 (excitation, 450–490 nm; emission 515– ∞ nm) for DHE, and filter set 20HE (exc.: 546/12 nm, em.: 607/80 nm) for AR. Pixel intensities were measured in area of circles using Axiovision Rel. 4.8 software (Carl Zeiss). The radii of circles were set to cover the largest sample area of the meristematic zone of the root apices and were not modified during the experiments.

2.6.2. Evaluation of enzymatic and non-ezymatic antioxidants in roots and cotyledons

Six replicates of 100 mg fresh material (roots or cotyledons) were homogenized with 1.4 mL cool phosphate buffer (0.1 M K_2HPO_4 buffer, pH 7.6 plus 0.1 mM EDTA) and centrifuged for 10 min at 12,000 × *g*. A Thermo Scientific GENESYS 10S UV–Visible Spectrophotometer was used for these measurements.

In order to evaluate protein concentration the samples were measured spectrophotometrically at 750 nm using the method of Lowry et al. (1951). These data were used to calculate the total superoxide dismutase (SOD) and catalase (CAT) activity. Total SOD (EC 1.15.1.1) activity was measured using the assay described by Misra and Fridovich (1972). The reaction mixture consisted of 1.4 mL 0.05 M (pH 10.2) buffer (Na_2CO_3, $NaHCO_3$, EDTA), 50 μL plant sample and 50 μl adrenaline. The absorbance was measured at 480 nm for 4 min. The activity was expressed as units (U) as unit/mg protein; and one unit of enzyme was defined as the amount that inhibits the formation of adrenochrome from adrenaline by 50%. The activity of CAT (EC 1.11.1.6) was determined according to the method of Beers and Sizer (1952). The mixture contained 0.05 M (pH 7.0) buffer (KH_2PO_4, Na_2HPO_4), 30 mM H_2O_2 and plant aliquot. One unit (U) of the enzyme was define-d as the amount that decomposes 1 μmol of H_2O_2/min /mg protein at 25 °C. Data are given in U/mg protein.

For the quantification of the contents of AsA and GSH, 250 mg plant material (roots or cotyledons) was grounded with 1 mL of 5% (v/v) trichloroacetic acid (TCA) and centrifuged (20 min, 9300 × *g*) then the supernatant was used to the measurements. For the determination of ascorbate/dehydroascorbate (AsA/DHA) content we used the method of Law et al. (1983). Spectrophotometric detections were executed at 525 nm. AsA/DHA contents are expressed in μmol/g fresh weight. The measurement of total glutathione content was performed at 412 nm following the method of Griffith (1980). Data are given as nmol/g fresh weight.

2.6.3. Evaluation of lipid peroxidation and protein carbonylation

At each treatment six replicates of 0.1 g fresh material (roots or cotyledons) were homogenized with 1.4 mL cooled phosphate buffer (0.1 M K_2HPO_4 buffer, puriss., pH 7.6 plus 0.1 mM EDTA) in a cold mortar and centrifuged for 10 min at 12,000 × *g*. In order to estimate the level of lipid peroxidation (LP; modified method of Placer et al., 1966) we determined the concentration of thiobarbituric acid reactive substances (TBARS) which are formed in the reaction between malondialdehyde (MDA), a member of the lipid peroxidation products and thiobarbituric acid (TBA). Therefore we mixed 0.5 mL of plant homogenate (supernatant) with the mixture of 15% (w/v) TCA (trichloroacetic acid, VWR), 0.375% (w/v) TBA (thiobarbituric acid, Merck-Sigma Group) and 0.25 M HCl (hydrochloric acid, Merck-Sigma Group). This mixture was heated for 15 min at 100 °C and cooled in ice for 15 min, then centrifuged for 5 min at 12,000 × *g*. We measured the absorbance of the supernatant at 532 nm. TBARS content was determined and is expressed in nmol/g fresh weight.

Carbonyl groups added to proteins during oxidative reactions were examined with Abcam's oxidized protein assay kit (ab 178020) with slight modifications of the manufacturer's instructions. Plant material (roots and cotyledons) was homogenized with 1 × extraction buffer containing 50 mM dithiothreitol. Samples were incubated on ice for 20 min, then centrifuged at 18,000 × *g* for 20 min at 4 °C. The measurement of protein content was executed using Bradford protein assay. For the derivatization reaction two 10 μL aliquots were used. First aliquot was treated with 10 μL 12% sodium dodecyl sulfate (SDS), then 20 μL 1 × 2,4-dinitrophenylhydrazine (DNPH) solution was added. The reaction was stopped after 15 min with 20 μL neutralization solution and was ready for gel electrophoresis. The second aliquot served as negative control, where instead of 1 × DNPH solution 20 μL of 1 × derivatization control solution was added. 7.5 μg of derivatized or non-derivatized control protein samples were separated on 12% SDS-PAGE gels, and transferred to PVDF membrane using tank transfer technique (25 mA, 16 h). Membranes were blocked for 1 h in blocking buffer (1 × PBS, pH 7,5 with 0.05% Tween 20 and 5% non-fat milk) and assayed with 1 × primary anti-DNP antibody (1:5000) for 3 h at room temperature. Membranes were washed three times with 1 × PBS-T, and then secondary antibody assay was performed with goat anti-rabbit IgG–alkaline phosphatase secondary antibody (1:10,000). Signal development was done with Immobilon Western Chemiluminescent HRP substrate

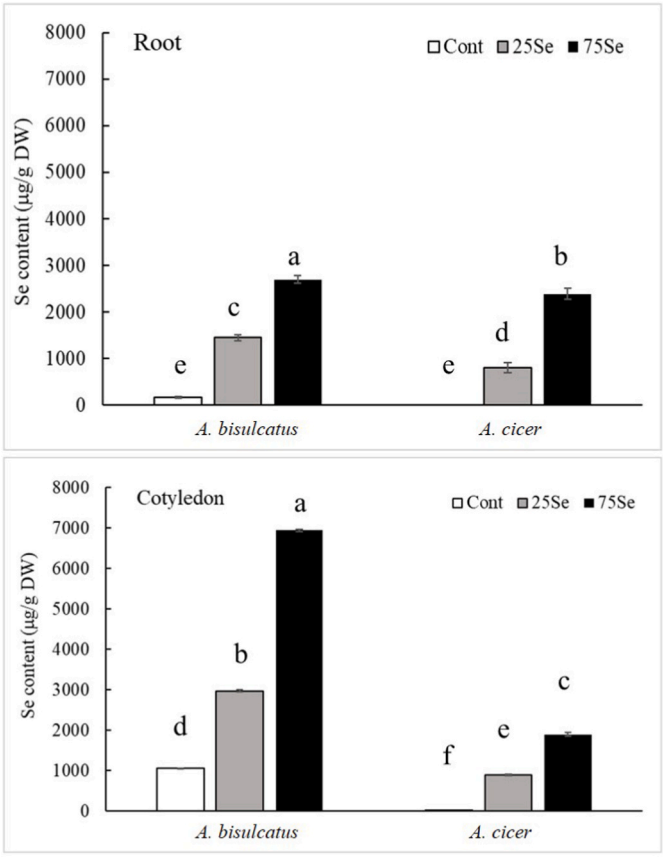

Fig. 1. Se content in the roots and cotyledons of 14-day-old *A. bisulcatus* and *A. cicer* treated with 0 (control, Cont), 25 μM (25Se) or 75 μM (75Se) sodium selenate for 14 days. Different letters indicate significant differences according to Duncan's test (n = 3, $p < 0.05$).

(Millipore Corporation, U.S.A.) using the manufacturer's DNP-labelled protein as positive control, and visualized by gel documentation system (Image System Felix 1000/2000, Biostep, Burkhardtsdorf, Germany).

2.7. Statistical analysis

Data are given in mean values ± standard error (SE). Statistical analysis was carried out using Excel 2016 and STATISTICA 14.0 softwares. Two-way analysis of variance (ANOVA) with Duncan's post-hoc test was applied to ascertain the effects of selenate treatment on parameters examined and to test the differences of means. Significant differences in some cases (Se content, GP, FW, DW, PRL, GSH and AsA) were indicated with lowercase letters at $p < 0.05$, while when the results were given in the form Control% significant alterations were expressed using asterisks at *$p < 0.05$, **$p < 0.01$ and ***$p < 0.001$ and n.s. = non-significant.

3. Results and discussion

3.1. Se is accumulated in the cotyledons of A. biculcatus and also in the cotyledons of A. cicer

In the roots of *A. bisulcatus*, 25 μM Se supplementation resulted in a 9-fold increase in Se content, while 75 μM Se provoked a 17-fold accumulation compared to control (Fig. 1A). Furthermore, quite high amount of Se (163 μg/g DW) was detected even in control roots probably due to the presence of Se within the seeds of this species (Freeman et al., 2006, Fig. 1A). On the contrary, in control roots of *A. cicer*, Se was not detectable. Similar to *A. bisulcatus*, the increasing dosage of exogenous selenate caused a significant elevation of Se content in the roots of *A. cicer* (Fig. 1A), which was confirmed also by Spearman's correlation coefficient (r = 0.96***). Surprisingly, Se concentration of 75 μM Se-treated *A. cicer* roots was above 2000 μg/g DW. Also in the case of *A. bisulcatus* cotyledons, Se accumulation was dose-dependent (Spearman's r = 0.95***), and the values were 2- and 3-fold higher at 25 and 75 μM Se compared to those of the roots (Fig. 1B). Moreover, the translocation factors of Se-exposed *A. bisulcatus* were above the value of 1 supporting the effective root-to-shoot Se translocation (Table 1). Beyond the efficient translocation, the high tissue Se concentration (~7000 μg/g DW) in the cotyledons of Se-treated *A. bisulcatus* also supports the hyperaccumulating nature of this species (Kikkert and Berkelaar, 2013; Raina et al., 2020). In the cotyledons of *A. cicer*, endogenous Se contents were similar to those of the roots and were significantly lower than in *A. bisulcatus* cotyledons (Fig. 1B). At 75 μM selenate supplementation, tissue Se content exceeded 1000 μg/g DW in *A. cicer*. Although, *A. cicer* was formerly described as a non Se accumulating species (Wang et al., 1999; Sors et al., 2009), our findings suggest that it accumulates Se in its aerial parts (Fig. 1B). At the same time, the translocation factor of 75 μM Se treated *A. cicer* were <1 (Table 1), which indicates that this species really cannot be considered as a hyperaccumulator.

Table 1
Translocation factors of control (Cont), 25 or 75 μM selenate treated *Astragalus bisulcatus* and *Astragalus cicer* seedlings. In the roots of control *A. cicer*, the Se concentration was not detectable therefore translocation factor was not calculated. N.D. = non-determined.

Translocation factors	Cont	25Se	75Se
A. bisulcatus	6.5	2.0	2.6
A. cicer	N.D.	1.1	0.8

Overall, both *Astragalus* species absorbed selenate from the growth medium and the rate of Se accumulation was shown to be dependent on both the organ, the species and the Se concentration applied. Interestingly, *A. cicer* seedlings showed notable Se accumulation in the aboveground tissues, but it was slighter than in *A. bisulcatus* (Fig. 1) and based on its Se translocation capacity (Table 1) it is not a hyperaccumulator species (Pasricha et al., 2021).

3.2. Exogenous Se exerts no effect on germination, but modifies the growth of Astragalus seedlings

In regard to germination percentage (GP) Se treatment caused no significant differences in *A. bisulcatus* or in *A. cicer* (Fig. 2A). However, in our former test the GP of the sensitive *A. membranaceus* was strongly inhibited by the applied Se concentration (Kolbert et al., 2018). Here, it seems that Se application had no dose-dependent effect on germination success probably due to the presence of the hard seed coat or the different sensitivity of *A. cicer* compared to *A. membranaceus* (Soltani et al., 2020). Nevertheless, control and 75 μM Se-treated seeds of *A. bisulcatus* germinated at significantly higher rate than those of *A. cicer* (Fig. 2A). Selenate application caused significant increment of the FW in case of 14-day-old *A. bisulcatus* seedlings (Fig. 2B). In contrast, the fresh biomass production of *A. cicer* plants was negatively affected by both Se concentrations. Similarly, in our previous study (Kolbert et al., 2018), the root and shoot FW of sensitive *A. membranaceus* remarkably reduced due to the presence of selenate. The FW of both untreated and Se-treated *A. cicer* plantlets proved to be significantly smaller than that of *A. bisulcatus* (Fig. 2B). Dry weights of the seedlings were not significantly influenced by Se treatments, but the DW of control and Se-exposed *A. cicer* was lower than that of *A. bisulcatus* (Fig. 2C). Primary root length was significantly affected by selenate supplementation only in case of *A. cicer* (Fig. 2D). At the same time, PR elongation of *A. bisulcatus* was shown to be unaffected by Se treatment due to the Se tolerance of

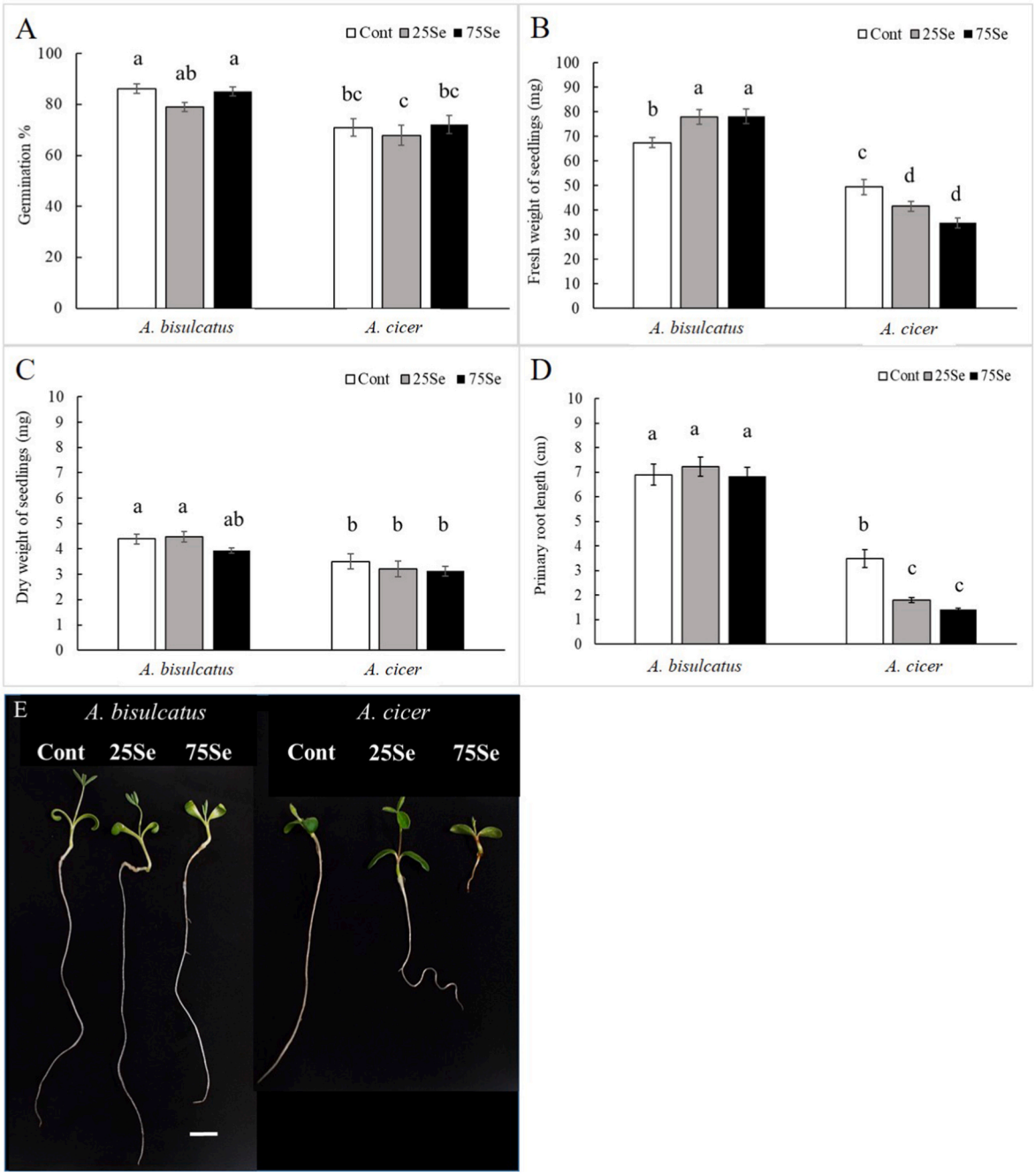

Fig. 2. (A) Germination percentage of *Astragalus bisulcatus* (*A.bis*) and *Astragalus cicer* (*A.cic*) on agar media supplemented with 0 (control, Cont), 25 or 75 μM sodium selenate. Fresh weight (B) and dry weight (C) of 14-day-old plants treated with 0 (control), 25 or 75 μM selenate. Different letters indicate significant differences according to Duncan's test (n = 25, $p < 0.05$). (E) Representative images of 14-day-old Astragalus plantlets grown on control or 25 or 75 μM selenate-containing agar media. Scale bar = 1 cm.

Table 2
Inhibition (%) of fresh weight (A) and primary root (PR) length (B) of *Astragalus bisulcatus* and *Astragalus cicer* grown in the presence of 25 or 75 μM selenate.

A) Inhibition of FW (%)	25Se	75Se
A. bisulcatus	−15.45	−15.67
A. cicer	15.89	29.40
B) Inhibition of PR length (%)	25Se	75Se
A. bisulcatus	−4.87	0.98
A. cicer	48.39	59.86

this species (Kolbert et al., 2018). The impact of exogenous Se on PR length was expressed as Se tolerance index according to Tamaoki et al. (2008), and it was around or above 100% in case of *A. bisulcatus* (data not shown). Basically, *A. cicer* had much shorter roots and both Se dosage significantly inhibited PR elongation which refers to the Se sensitivity of this species. These findings are represented in Fig. 2E. Since the biomass of healthy individuals of the two species was notably different, the degrees of Se-induced inhibition (%) in the case of primary root length and fresh weight were calculated (Table 2). Both the raw data and the inhibition % clearly show that Se exposure exerts a dose-dependent negative effect on the biomass production of *A. cicer* seedlings, while in the case of *A. bisulcatus* there is no Se-related

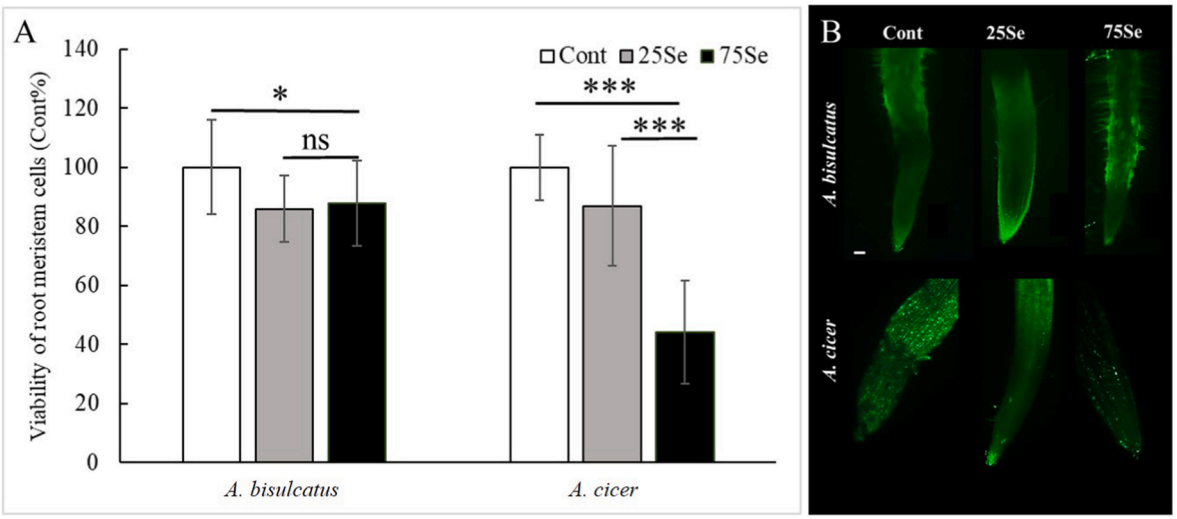

Fig. 3. (A) Cell viability of root meristematic cells in control and Se-treated (25 or 75 μM selenate) *Astragalus bisulcatus* (*A.bis*) and *Astragalus cicer* (*A.cic*). Control values are regarded to be 100% and all data are given as the percentage of control. Different letters indicate significant differences according to Duncan's test ($n = 16$, $p < 0.05$). (B) Representative fluorescent microscopic images showing root tips of control (Cont) and selenate-treated *Astragalus* species labelled with fluorescein diacetate (FDA). Scale bar = 100 μm.

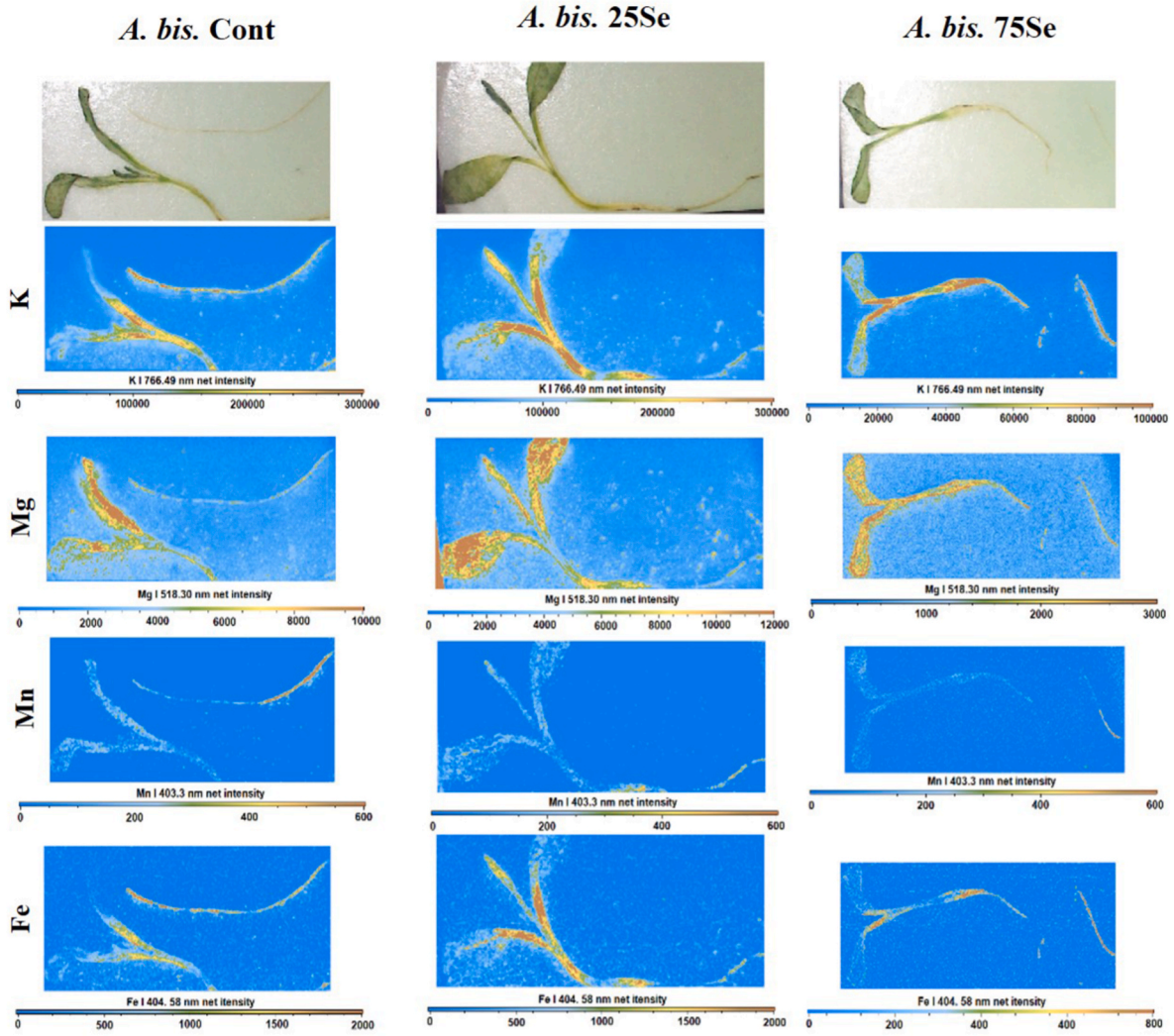

Fig. 4. LIBS elemental maps demonstrating the *in planta* distribution of selected macro- and microelements in *Astragalus bisulcatus (A. bis.)* seedlings cultivated on the media with 0 (control, Cont), 25 μM (25Se) and 75 μM (75Se) selenate for 14 days.

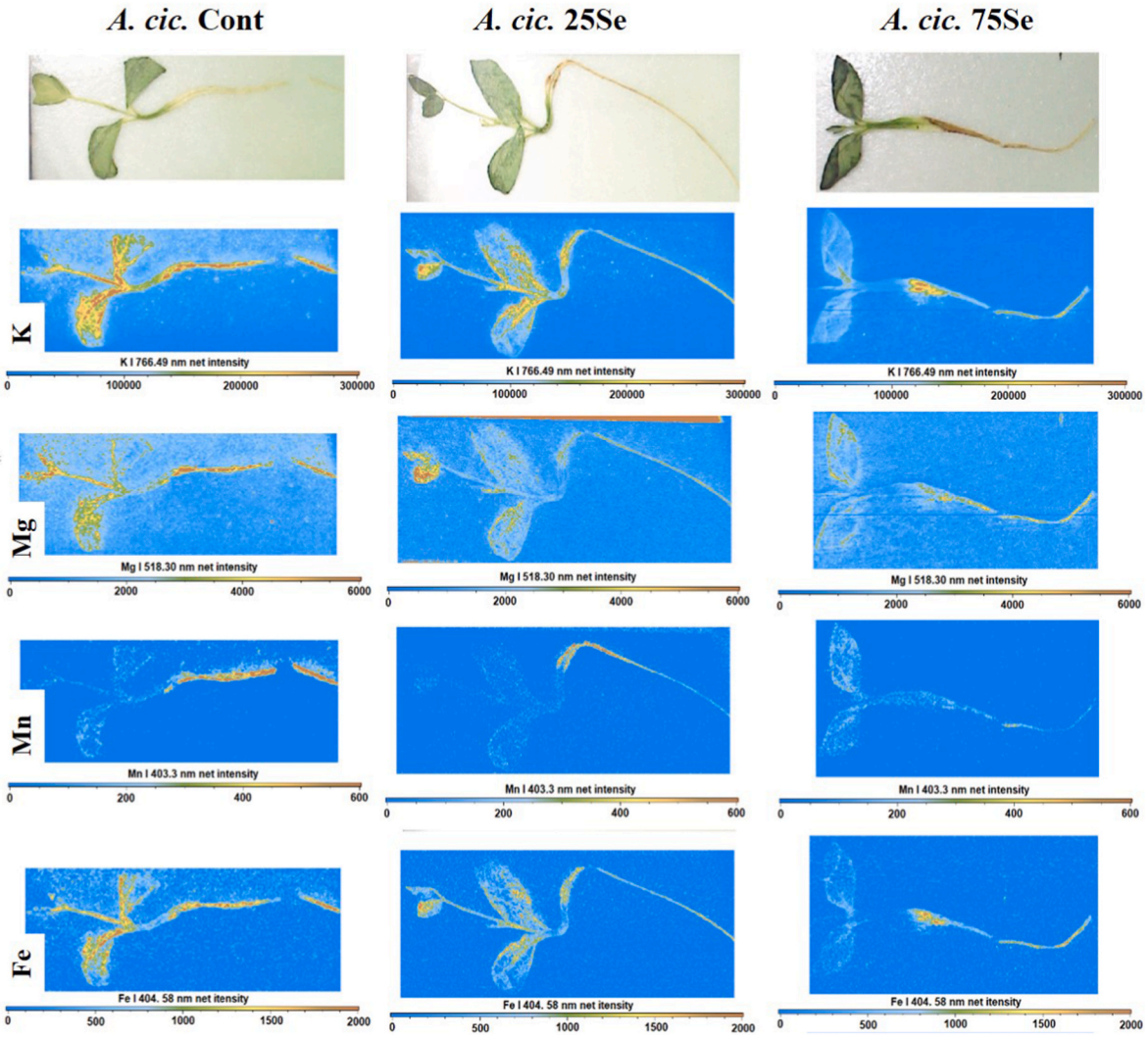

Fig. 5. LIBS elemental maps showing *in planta* distribution of macro- and microelements in *Astragalus cicer (A. cic.)* seedlings cultivated on the media with 0 (control, Cont), 25 μM (25Se) and 75 μM (75Se) selenate for 14 days.

inhibition (in fact, there is stimulation).

In accordance with the PR length data, the meristem cells of *A. bisulcatus* root tips showed only a moderate viability loss due to 25 or 75 μM selenate exposure compared to control (16% and 12%, respectively, Fig. 3AB). Whilst, root elongation of *A. cicer* was negatively affected by both applied Se doses (Fig. 2D), remarkable loss of root meristem cell viability (56%) was recorded only at the highest Se concentration (Fig. 3B) which suggests that other internal factors (*e.g.* disturbed hormonal balance) may contribute to the inhibited root elongation (Ağar et al., 2006; Van Hoewyk et al., 2008; Lehotai et al., 2012; Ardebili et al., 2015; Hawrylak-Nowak, 2022). Based on the biomass and root cell viability data, at their post-germination stage *A. cicer* is sensitive to the presence of Se in the growth medium, while *A. bisulcatus* tolerates both Se concentrations.

3.3. Se supplementation modifies the distribution of macro- and microelements within the seedlings

Excess Se has been shown to modify macro- and microelement homeostasis of plants (Tobiasz et al., 2014; Kolbert et al., 2018) and not only their content might be affected but also their *in planta* distribution. In case of *A. bisulcatus,* despite the high tissue Se content, no significant changes in macroelements such as potassium (K) and magnesium (Mg) content was observed (Fig. 4). Moreover, 75 μM Se induced only a slight decline of microelement *viz.* iron (Fe) and manganese (Mn) signals (Fig. 4). The slightly affected macro- and microelement contents support the Se tolerance of *A. bisulcatus*.

As shown in Fig. 5, the amounts of K, Mg, Mn and Fe decreased in *A. cicer* plantlets as the effect of the elevating Se concentrations. Furthermore, signals corresponding to Fe, K and Mg were found dominantly in the „shoot" (hypocotyl together with cotyledons) in control and 25 μM Se-supplemented *A. cicer* plants, while Mn was detected in the roots (Fig. 5) indicating that the distribution of these macro- and microelements is different. As a result of 75 μM Se addition Fe, K and Mg levels notably reduced in the shoot and signals were detected only in the root. In case of Mn, the signal remarkably reduced in the whole seedling as the effect of 75 μM Se (Fig. 5). Results of the LIBS analysis show that the distribution of the examined macro- and microelements has significantly changed due to Se addition especially in *A. cicer* seedlings which reflects to a modified nutritional status of the treated plants. The insufficient amount of essential nutrients probably contributes to the reduction of biomass production of *A. cicer* (Fig. 2). In a former study, Filek et al. (2010) observed that in 14-day-old rapeseed (*Brassica napus*) seedlings grown on MS medium containing 100 μM or 200 μM selenate, K and Mg content of both shoot and root decreased, and Mn and Fe homeostasis is also disturbed. Thus, previous observations where Se-induced imbalance of nutritional status in *Arabidopsis*, rapeseed and wheat (*Triticum aestivum*) has been evaluated by inductively coupled

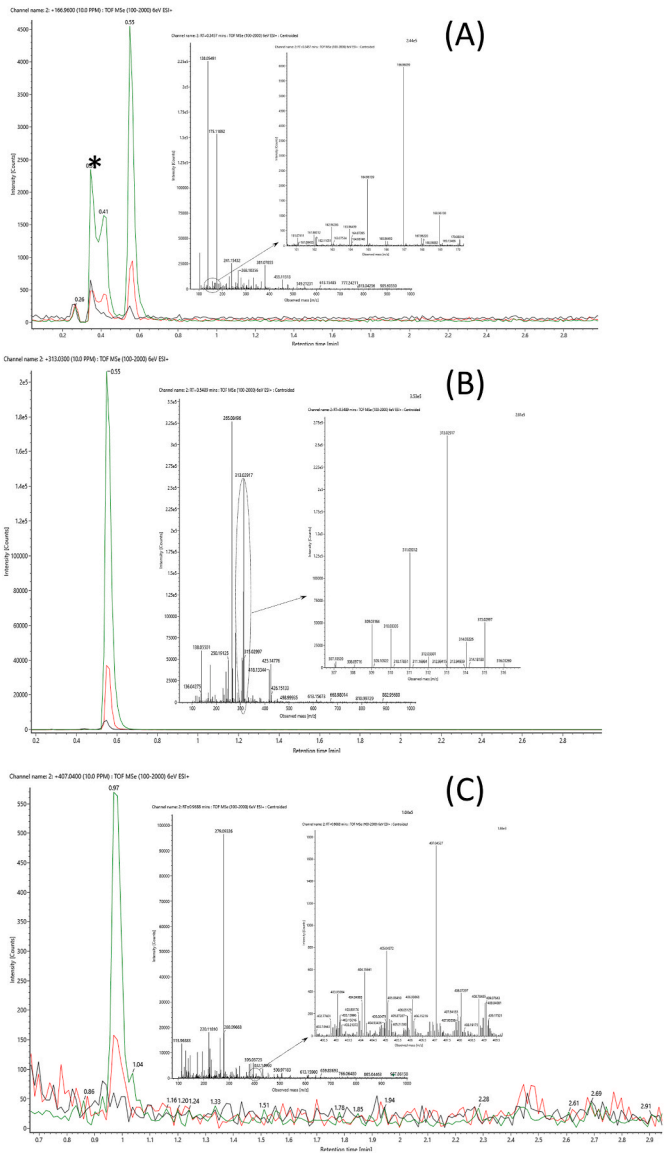

Fig. 6. LC-Unispray-QTOF-MS extracted ion chromatograms of the extracts prepared from the cotyledons of 14-day-old control (black trace) and Se-treated (25 μM and 75 μM selenate; red and green traces, respectively) *A. bisulcatus* seedlings. Subfigure (A) shows the presence of methyl-selenocysteine (MetSeCys; '*' indicates the elution at 0.35 min, assigned with the help of the characteristic in-source fragment at *m/z* 166.96), (B) refers to γ-glutamyl-methyl-selenocysteine (γ-Glu-MetSeCys; elution at 0.55 min; note also the characteristic in-source fragment at *m/z* 166.96 at 0.55 min in subfigure (A)), while (C) presents that the tentative Se-sugar (at 0.97 min) was detected only in the case of the 25 μM and 75 μM selenate treatments. The insets show the full scan spectra at the apexes, together with the relevant isotopologue patterns of the Se-species detected.

plasma optical emission and mass spectrometry methods (Feng et al., 2009; Filek et al., 2010; Ribeiro et al., 2016) support our results. Furthermore, the LIBS approach provides spatial information about the distribution of macro- and microelements and it is suitable for the visualization of macro- and microelement distributions in plantlets of Se accumulator species.

3.4. Se-treated A. bisulcatus produces methylated selenospecies and a tentative selenosugar

The results of the LC-Unispray-QTOF-MS analysis exhibited notable changes more in cotyledons than in roots. Methylated derivatives of selenocysteine (SeCys) such as methyl-selenocysteine (MetSeCys, Fig. 6A) and γ-glutamyl-methyl-selenocysteine (γ-Glu-MetSeCys, Fig. 6B) were detected in the cotyledons of both control and Se-treated *A. bisulcatus* seedlings. MetSeCys did not occur in the roots (neither in the control nor in the treated samples) of *A. bisulcatus* seedlings. This phenomenon is common in Se-hyperaccumulators since MetSeCys is the precursor of volatile dimethyl diselenide (DMDSe) found in hyperaccumulators, and its derivative γ-Glu-MetSeCys can be stored in various organs of Se-hyperaccumulators (Sors et al., 2009; Shahid et al., 2018; Kurek et al., 2020; Ponton et al., 2020). Unlike our results, Valdez Barillas et al. (2012) collected *A. bisulcatus* plants in their natural habitats to determine Se speciation using X-ray absorption near-edge structure spectroscopy (μXANES) and they found that in the cortex of the taproot ca. 90% of Se was in an organic C–Se–C form, probably as MetSeCys, γ-Glu-MetSeCys, selenocystathione and/or selenomethionine. This contradiction is likely due to the different ages and growth conditions of plants.

Furthermore, in the cotyledons of *A. bisulcatus* treated with 75 μM Se the amount of γ-Glu-MetSeCys was present in approx. 40-fold higher concentration, compared to the roots (Fig. 7A). Interestingly, a selenium containing disaccharide (that is, a tentative selenosugar with the neutral composition of $C_{12}H_{22}O_{10}Se$) was also detected in *A. bisulcatus* cotyledons and roots, but only when selenate was added to the cultivation medium (Fig. 6C) and it was two-fold more abundant in cotyledons than in roots (Fig. 7B). This finding is in accordance with the formerly reported statement by White (2017) that in the hyperaccumulator *A. bisulcatus*, the genes of selenocysteine methyltransferase producing MetSeCys and the unknown enzyme producing γ-Glu-MetSeCys (Trippe and Pilon-Smits, 2021) work constitutively. Meanwhile, we might suppose that either the genes responsible for selenosugar production are facultative, and the generation of selenosugars also contributes to the Se detoxification process (Aureli et al., 2012; Ouerdane et al., 2020) or the formation of selenosugars is driven only by the high reactivity of selenium, that is, in a non-enzymatic way.

At the same time, no organic Se forms could be detected either in the roots or in the cotyledons of control or Se-treated *A. cicer* planlets. When Sors et al. (2005) analyzed Se assimilation in various *Astragalus* species, they could detect a much lower concentration (~14 nmol/g FW) of MetSeCys in the shoots of *A. cicer* compared to that of *A. bisulcatus* (~252 nmol g/FW). We might suppose that in our case, Se which accumulated in the cotyledons of *A. cicer* was likely present as inorganic selenate and elemental Se (Se^0) (Wang et al., 1999; Sors et al., 2009; Statwick et al., 2016).

3.5. Exogenous Se affects ROS and H_2S levels in the root tips of Astragalus species

It is well-known that Se shows dual behavior, *i.e.* at smaller doses it exerts antioxidant effect, while at higher amounts it provokes the overproduction of ROS (summarized by Van Hoewyk, 2013; Gupta and Gupta, 2017). However, the antioxidant or pro-oxidant nature of Se depends not only on its concentration but also on the Se-tolerance of the plant species (Van Hoewyk, 2013). In the roots of *A. bisulcatus*, the lower selenate concentration (25 μM Se) proved to be beneficial provoking a significant decline of superoxide anion levels compared to the control, while in case of higher Se (75 μM) dose, superoxide level was similar to that of control plants (Fig. 8A). Interestingly, in *A. cicer* roots, the applied selenate had no effect on superoxide anion level (Fig. 8A). In the root apexes of *A. bisulcatus*, the H_2O_2 levels were decreased by 73% and 60% compared to the control in case of 25 and 75 μM Se treatments, respectively (Fig. 8B). In contrast, in *A. cicer* roots, selenate addition exerted no effect on H_2O_2 levels (Fig. 8B). Our results are supported by Se-induced depletion of ROS forms in cowpea (*Vigna unguiculata*, Lapaz et al., 2019) and radish (*Raphanus sativus*, Amirabad et al., 2020). Furthermore, in *A. bisulcatus*, the low Se dosage might be beneficial due

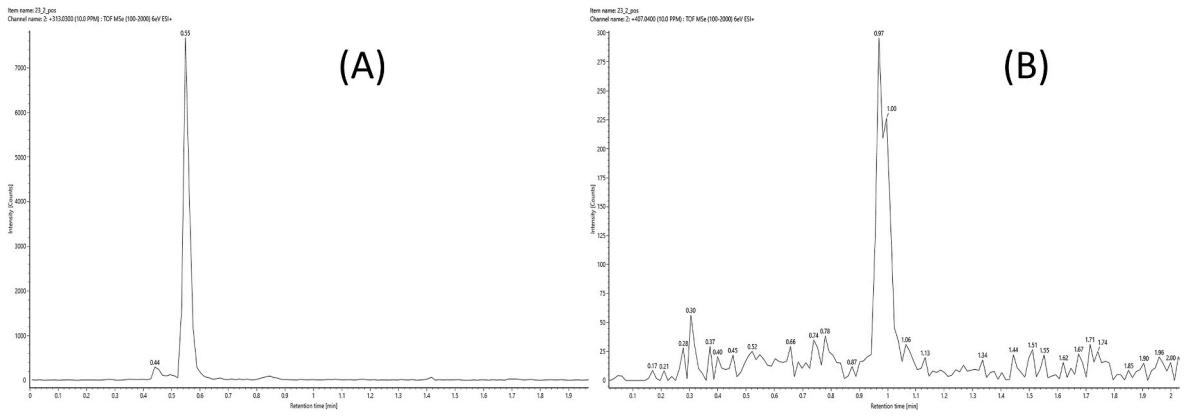

Fig. 7. LC-ESI-QTOF-MS extracted ion chromatograms of the extracts prepared from the roots of 14-day-old, 75 μM selenate treated *A. bisulcatus* seedlings. Subfigure (A) refers to γ-glutamyl-methyl-selenocysteine (γ-Glu-MetSeCys), while (B) shows the elution of the tentative Se-sugar (at 0.97 min).

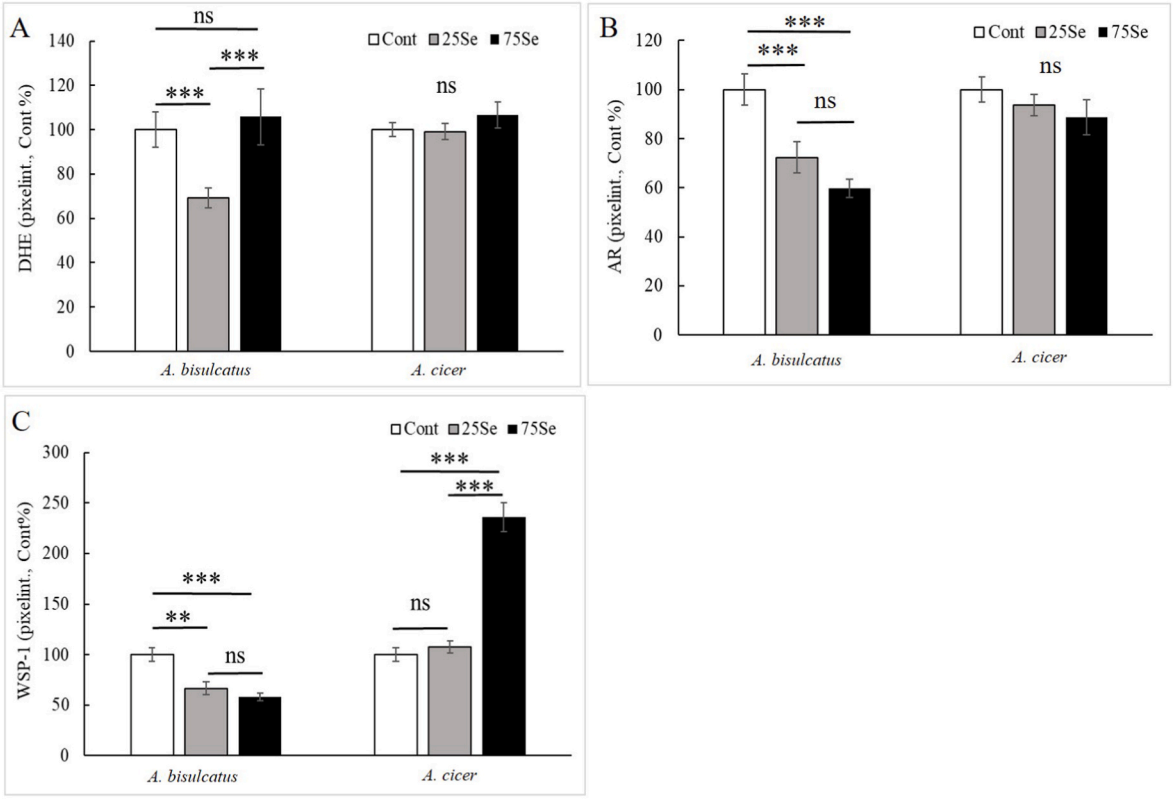

Fig. 8. Superoxide radical levels (A) detected by DHE and hydrogen peroxide levels (B) determined by AR staining in the root tips of selenate-treated *Astragalus biculcatus (A.bis)* or *Astragalus cicer (A.cic)*. Endogenous H_2S levels (C) in selenate-treated *Astragalus* root apexes determined and visualized using WSP-1 probe. Control values are regarded to be 100% and all data are given as the percentage of control. Asterisks indicate significant differences between Se-treated (25 or 75 μM) and control plants within the same species according to Duncan's test (n = 10, * at $p \leq 0.05$; ** at $p < 0.01$ and *** at $p < 0.001$ significance level; ns = not significant).

to the reduction of physiological ROS levels. At the same time, persistently elevated ROS levels were not detected in the sensitive species either. The lack of significant ROS (superoxide radical or hydrogen peroxide) production in sensitive *A. cicer* was presumably due to the possibility that oxidative burst had happened earlier than our sampling. Namely, ROS accumulation might have occurred soon after selenate application and later it might have been attenuated. In the root tips of selenate-treated *A. bisulcatus*, H_2S-associated fluorescence showed a dose-dependent decrease, as is was confirmed by Spearman's correlation coefficient ($r = -0.75$***). However, in the root apexes of Se-sensitive *A. cicer* higher (75 μM) selenate induced a significant H_2S accumulation (Fig. 8C) compared to both control and 25 μM Se-treated plants. The WSP-1 fluorescence intensity measured at 75 μM Se was ~2.4-fold higher than that of control (Fig. 8C). Although, numerous results have presented that biotic and abiotic stressors have impact on H_2S level of plants or the activation of the antioxidant defense system triggerred by exogenous H_2S is responsible of the stress tolerance of plants (Hancock, 2019; Huang et al., 2021), there are only a few experimental data showing how exogenous Se affect endogenous H_2S content within roots. Chen et al. (2014) observed a dose-dependent reduction of H_2S in the root tips of *Brassica rapa* in the presence of selenite and this was accompained by root growth inhibition. We found

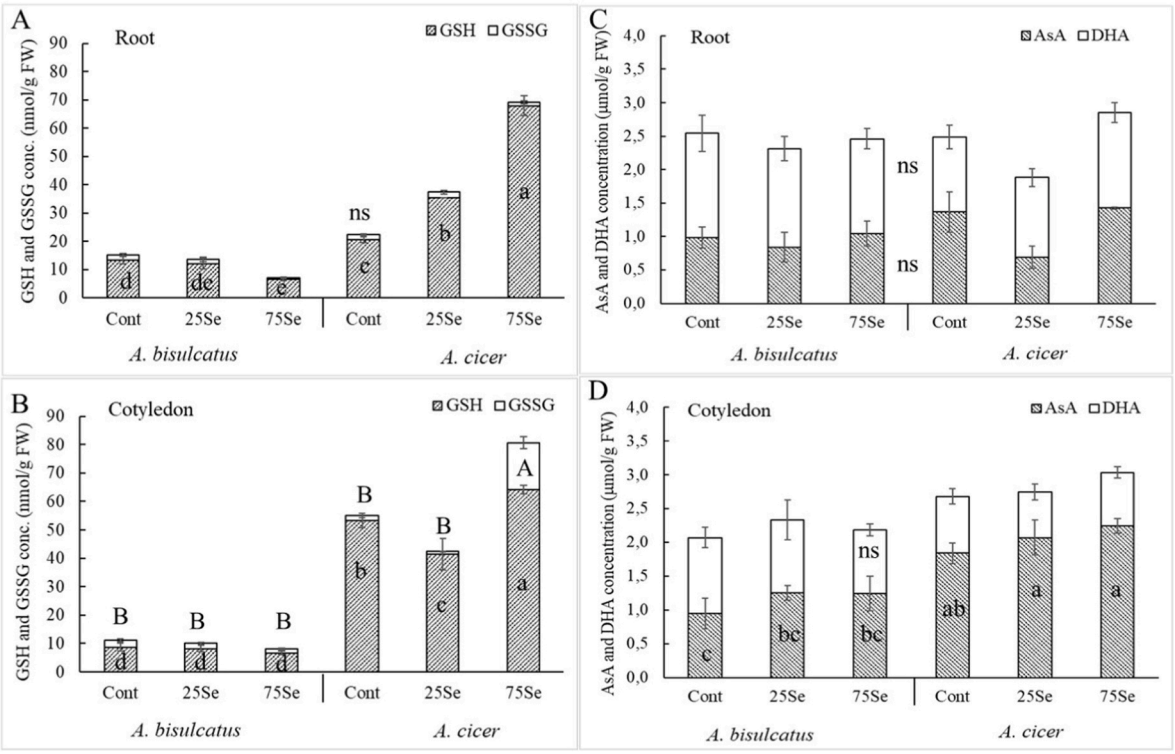

Fig. 9. Concentrations of GSH (reduced glutathione) and GSSG (oxidized glutathione) (nmol/g FW) and the concentrations of AsA (reduced ascorbate) and DHA (dehydroascrobate) (μmol/g FW) in roots (A, C) and cotyledons (B, D) of *Astragalus bisulcatus (A.bis)* and *Astragalus cicer (A.cic)* seedlings exposed to 0, 25 or 75 μM selenate. Different minuscules indicate significant differences among GSH values while capital letters refer to significant differences among GSSG values according to Duncan's test ($n = 3$, $p < 0.05$). In case of AsA and DHA different minuscules indicate significant differences among the values according to Duncan's test ($n = 3$, $p < 0.05$), ns = not significant.

similar changes in the root apexes of selenate-treated *A. bisulcatus* plants. The opposite changes in the root tips of *A. cicer*, might be in correlation with the different Se-tolerance of these species. Moreover, the root growth inhibition of *A. cicer* caused by the higher selenate dosage might be associated with its increased H_2S content, as it was demonstrated during various stress conditions (Cui et al., 2014; Fang et al., 2014; Yang et al., 2022).

3.6. Exogenous Se differently affects GSH and AsA contents in Astragalus seedlings

Surprisingly, GSH content in the control roots of *A. cicer* was significantly higher than that of *A. bisulcatus*. In the roots of *A. bisulcatus*, significant GSH (reduced glutathione) depletion (51%) was observed but only at 75 μM Se compared to control and it was confirmed also by Spearman's correlation coefficient ($r = -0.68^{**}$). Differently, in *A. cicer* roots selenate treatment enhanced GSH content in dose-dependent manner, namely 25 and 75 μM Se addition resulted in 1.7- and 3.3-fold increment regarding control values (Fig. 9A). Spearman's analysis also verified a significantly positive correlationship ($r = 0.95^{***}$) between exogenous Se dosage and the GSH content in the roots of *A. cicer*. GSSG (oxidized form of glutathione) content was low and unaffected in Se-treated roots of both species compared to control (Fig. 9A). In the roots of *A. bisulcatus*, selenate application had no impact on GSH:GSSG ratio while this ratio shifted toward the significant accrual of GSH in *A. cicer* roots due to both dosages of Se supply. The Se-induced increase in GSH content suggests the activation of GSH-associated antioxidant system contributing to the control of ROS levels in *A. cicer*. Unlike our results, Grant et al. (2011) found a positive correlation between the root length and GSH levels in selenate-treated *Arabidopsis thaliana* and stated that growth inhibition of the roots was the consequence of altered auxin accumulation and transport disturbed by reduced GSH levels. In a recent study on the transcriptomic, proteomic and metabolomic aspects of selenate toxicity in Se-hyperaccumulator *Cardamine violifolia,* it has been revealed that decreased biosynthesis of GSH under selenate stress was due to the expression changes of genes related to GSH metabolism (Rao et al., 2021). Based on this, it is conceivable that the reduction in GSH level of *A. bisulcatus* roots may be caused by the downregulation of GSH biosynthesis. At the same time, the reduction of selenate to selenite requires GSH (White, 2017) which may result in its decreased levels. In *A. cicer* cotyledons, total glutathione (GSH + GSSG) amount proved to be 5-10-fold higher compared to *A. bisulcatus* (Fig. 9B). Selenate did not influence either GSH or GSSG content in *A. bisulcatus* cotyledons. In contrast to this, in *A. cicer* cotyledons the lower selenate dosage caused a significant decrease in GSH content, while 75 μM Se significantly increased the concentration of both GSH and GSSG. The increase in the ratio of the oxidized form indicates that the redox state of cotyledon cells shifts toward the oxidation state, causing oxidative stress in *A. cicer*. Moreover, the Se-induced increase in GSH content may result from the upregulation of GSH biosynthesis enzyme genes (Maassoumi et al., 2022) or from the increase of glutathione reductase activity (Hassan et al., 2018). Additionally, the involvement of GSH-dependent reduction of selenate may be considered as a potential influencing factor of GSH level changes.

The concentration of AsA (reduced form of ascorbic acid) and DHA (dehydroascorbate) in the roots of both species proved to be unaffected by selenate supplement (Fig. 9C). In the roots of *A. bisulcatus,* the AsA:DHA ratios were within the range 0.7–0.9 indicating that the main part of the total ascorbate pool is in oxidized form. This suggests the involvement of AsA in the antioxidant defence of *A. bisulcatus*. On the other hand, AsA:DHA ratios in *A. cicer* roots were 1.5 and 1.0 in the case of control and 75 μM Se, respectively. This reflects that the reduced form is in the majority in the ascorbate pool (Fig. 9C). In cotyledons, Se addition did not cause significant differences in DHA contents of the

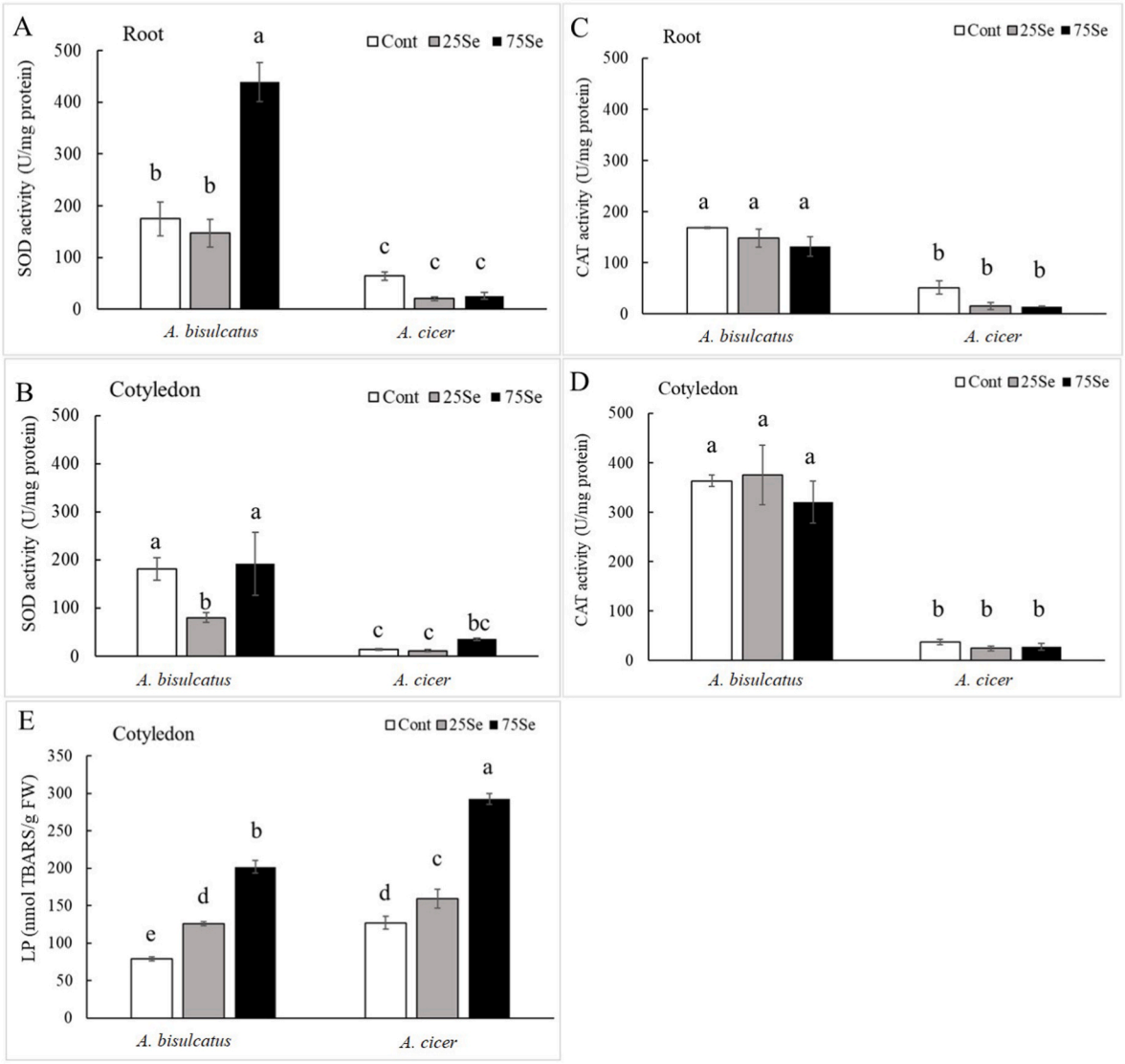

Fig. 10. Activity of superoxide dismutase (SOD, A, B) and catalase (CAT, C, D) (U/g fresh weight) in the root and cotyledons of 14-day-old *Astragalus bisulcatus (A. bis)* and *Astragalus cicer* (*A. cic)* seedlings grown in the absence (Cont) or in the presence of 25 or 75 μM sodium selenate. (E) The level of lipid peroxidation (LP, nmol MDA/g FW) in the cotyledons of *Astragalus* seedlings. Different letters indicate significant differences according to Duncan's test ($n = 4$, $p < 0.05$).

species (Fig. 9D). Interestingly, the AsA content of *A. cicer* cotyledons was significantly higher than that of *A. bisulcatus* even in control plants. Moreover, in the cotyledons of both species ascorbate was found to be predominantly in the reduced form (AsA) since almost all the AsA:DHA ratios were above 1.00, especially in case of *A. cicer,* those where the AsA:DHA ratios were within the range 2.3–4.4. Still AsA levels proved to be independent of exogenous Se dosage according to the correlation coefficients ($r = 0.16$ ns for *A. bisulcatus* and $r = 0.36$ ns for *A. cicer*, respectively). In previous studies, the effect of Se on AsA concentration proved to be diverse depending on the plant species because decreased, increased and unchanged AsA contents were measured in white mustard (*Sinapis alba*), alfalfa (*Medicago sativa*) and basil (*Ocimum basilicum*) (Woch and Hawrylak-Nowak, 2019; Ardebili et al., 2015), respectively. In our study, unlike the roots, the AsA:DHA ratios in cotyledons generally shifted toward AsA level, particularly in *A. cicer* which was probably due to the increased GSH content reducing DHA back to AsA in Halliwell-Asada-cycle (Foyer and Noctor, 2011; Halliwell, 2020). Beside the interspecies alterations, these changes of AsA:DHA ratios seem also to be organ-dependent, but it was more expressed in non-tolerant *A. cicer*.

3.7. Se differently modulates enzymatic antioxidants in Astragalus seedlings

Excess selenate has been reported to induce the activity of ROS-scavenging enzymes, like SOD, CAT or ascorbate peroxidase (APX) in a dose-dependent manner (Van Hoewyk, 2013). Here, the total activity of superoxide-eliminating SOD enzymes was control-like in case of 25 μM Se treatments, but significantly increased (2.5-fold compared to control) in the roots of 75 μM Se-exposed *A. bisulcatus* (Fig. 10A). In the roots of *A. cicer*, SOD activity seemed to be reduced by Se exposure, but the differences were not significant. It has to be noted that the values of SOD activity both in control and Se treated *A. cicer* were significantly lower compared to *A. bisulcatus* (Fig. 10A). In the cotyledons of *A. bisulcatus,* 25 μM Se significantly decreased total SOD activity (Fig. 10B), resulting in ~60% activity loss compared to untreated plants. The cotyledons of 75 μM Se exposed A. *bisulcatus* showed control-like SOD activity (Fig. 10B). Similar to the roots, SODs showed significantly lower activity in *A. cicer* cotyledons relative to *A. bisulcatus* and Se exposure did not significantly modify their activity (Fig. 10B). Results show that in *A. bisulcatus* only 75 μM selenate could intensify SOD activity but only in root, while in cotyledons SOD activity declined due to

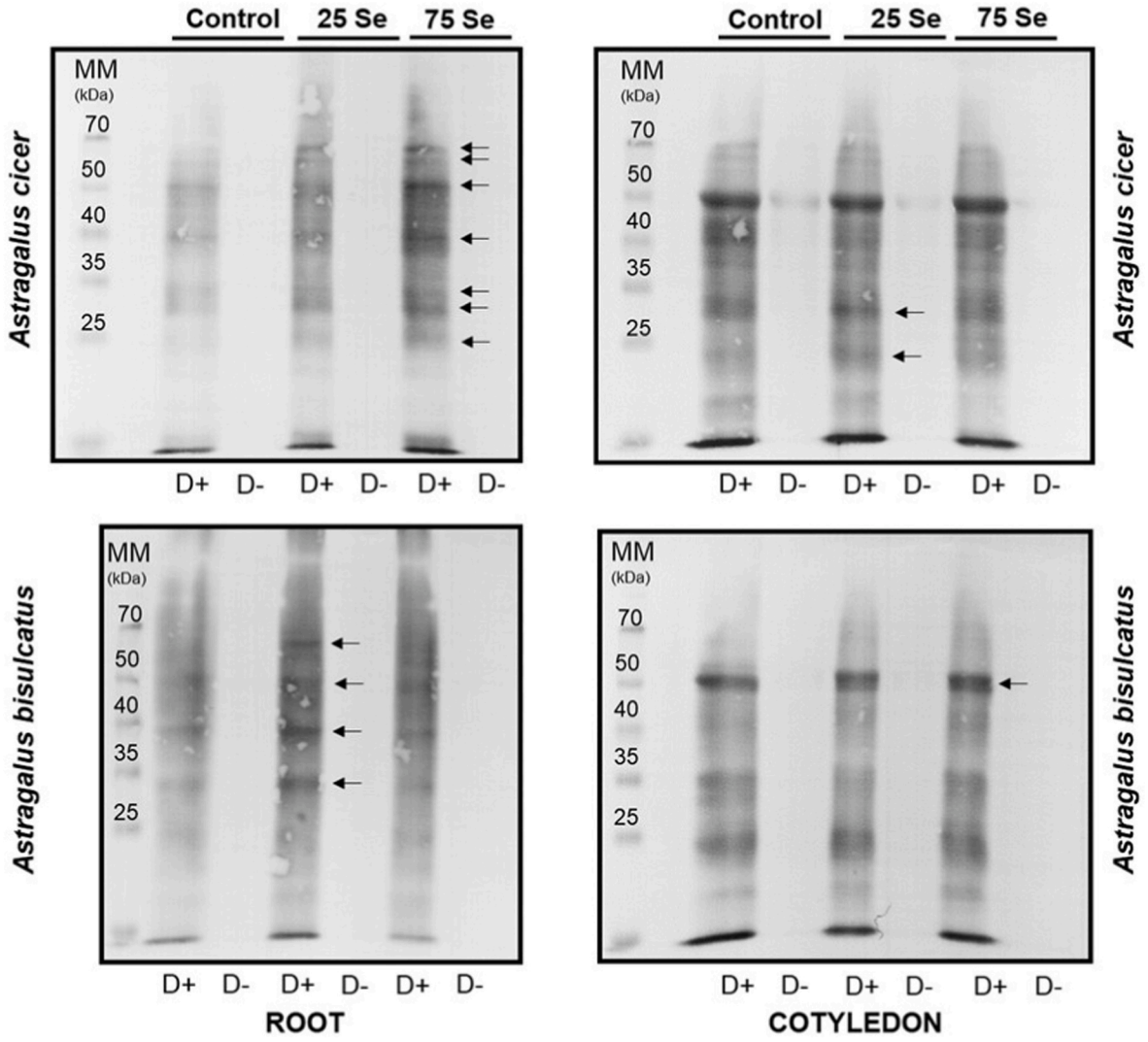

Fig. 11. Representative immunoblots probed with anti-DNP antibody (1:5000) showing protein carbonylation in the roots and cotyledons of 14-day-old *Astragalus cicer* and *Astragalus bisulcatus* seedlings exposed to 0, 25 or 75 μM selenate. Protein bands with intensified signal compared to control are marked with black arrows. MM = molecule marker, D+ = derivatized sample, D- = non-derivatized sample.

lower Se which refers to organ-dependence of the Se-triggered response in SOD activity. In *A. cicer,* selenate treatment had no effect on SOD functionality. Dissimilar to our results, Ramos et al. (2010) detected induced SOD activity at low selenite concentrations (up to 32 μM) but decreased activity at higher Se concentration in lettuce (*Lactuca sativa*) leaves. Additionally, Gouveia et al. (2020) observed that toxic dosage of selenate (1.5 mM) significantly increased SOD activity in hydroponically treated rice (*Oryza sativa*) seedlings. Based on our findings we suppose that the reduced activity of SOD enzymes of *A. cicer* may contribute to its relative sensitivity.

As for CAT, *A. bisulcatus* exhibited significantly higher activity compared to *A. cicer*, both in the roots and cotyledons (Fig. 10C and D). The interspecies difference was more expressed in cotyledons, since CAT activity of *A. bisulcatus* were 10-15-fold higher than those of *A. cicer* (Fig. 10D). The enzyme activity was not influenced by selenate addition in either organ of either species. However, the reduced H_2O_2 content of *A. bisulcatus* (Fig. 8B) can possibly be due to consequence of the elevated activity of other H_2O_2-eliminating enzymes like glutathione proxidase or APX as it was found in rice (Du et al.,2019; Gouveia et al., 2020; Das et al., 2020). Our results allow us to speculate that Se-tolerance of *A. bisulcatus* may be associated with the elevated basal CAT activity mainly in the cotyledons where the major portion of Se is accumulated (Fig. 1B), and Se-sensitivity of *A. cicer* may be associated with its low CAT activity.

Selenate treatment differently affected LP in *Astragalus* species, predominantly in cotyledons (Fig. 10E). In the roots of the species, neither low (25 μM) nor high (75 μM) Se concentration modulated LP values in comparison with control (data are not shown). Similar to this, TBARS concentration of roots remained unchanged when lettuce was subjected to 2–15 μM selenate during hydroponic cultivation (Hawrylak-Nowak, 2013). In the cotyledons of *A. bisulcatus*, LP levels showed an increase in a concentration-dependent manner as the effect of Se addition (confirmed by Spearman's correlation analysis, $r = 0.95^{***}$). At the same time, TBARS contents of *A. cicer* cotyledons were 2-3-fold higher than those of *A. bisulcatus*, both in control and Se-treated plants and Se supplementation caused a dose-dependent increase (Spearman's $r = 0.90^{**}$) (Fig. 10E). Based on these, selenate application exerts remarkable impact on LP levels in the cotyledons of both species. We may also assess that interspecies differences in LP occurred only in case of cotyledons independently of Se concentration. Numerous reports have shown that exogenous selenate may have dose-dependently dual effect on lipid peroxidation either in roots or leaves (Cartes et al., 2005; Ríos et al., 2008; Hawrylak-Nowak et al., 2015; Tian et al., 2017). Additionally, a positive correlation between the applied Se dosage and the

activity of glutathione peroxidase (GSH-Px) has been shown (Ríos et al., 2008; Maassoumi et al., 2022). In this case, TBARS content was much higher even in control cotyledons of *A. cicer* in comparison with *A. bisulcatus* which may contribute to the sensitivity of this species.

3.8. Se-induced protein carbonylation is dose- and organ-specific in Astragalus species

Beyond lipid peroxidation, the overproduction of ROS may result also in protein carbonylation (Matamoros et al., 2018). Due to the irreversible feature of protein carbonylation, the level of carbonyl-modulated proteins is considered to be a good indicator of the cells' oxidative status (Ciacka et al., 2020; Molnár et al., 2020). In the roots of *A. cicer,* selenate addition resulted in intense, concentration-dependent carbonylation of several protein bands compared to control (intensified immunopositive signals are indicated by arrows in Fig. 11, Fig. S1). In the roots of 25 μM Se-exposed *A. bisulcatus*, a remarkably stronger carbonylation signal was observed in at least four protein bands compared to control (indicated by arrows in Fig. 11, Fig. S1), while at 75 μM Se protein carbonylation was less pronounced but more intense compared to control (Fig. 11, Fig. S1) indicating a possible signalling role of low Se-induced protein carbonylation (Tola et al., 2021). In regard of cotyledons, a slight Se-triggered enhancement in carbonylation of two protein bands was detected in *A. cicer* (Fig. 11, Fig. S1). In case of *A. bisulcatus* cotyledons, both Se dosages triggered enhanced carbonylation in one protein band (Fig. 11, Fig. S1). Overall, the Se dose-dependent induction of protein carbonylation is more obvious in the roots than in the cotyledons of *A. cicer*. Since MDA (reactive carbonyl species) content was not increased in the roots, divalent metal ion catalyzed direct protein carbonylation may happen (Tola et al., 2021). The strong increase in shoot MDA content was accompanied by only a slight increase in carbonylation, but it is possible that the increase in the amount of LP-derived reactive carbony species indirectly contributes to the increase in protein carbonylation in the shoot of both species (Tola et al., 2021). If we compare the extent of protein carbonylation in the roots of the species in the presence of 75 μM Se, we may suppose a correlation between selenate sensitivity and the degree of protein carbonylation.

4. Conclusions

Grown on selenate-supplemented media, both *Astragalus bisulcatus* and *Astragalus cicer* accumulate Se in the aboveground tissues but only *A. bisulcatus* showed effective root-to-shoot translocation. The Se sensitivity of *A. cicer* was indicated by reduced seedling fresh weight, root growth and RAM viability in the presence of selenate. Furthermore, the disturbed distribution of selected macro- and microelements supports the Se sensitive nature of *A. cicer*. The lack of organic Se forms in *A. cicer* suggests that the majority of the accumulated Se may be present as inorganic forms, while in *A. bisulcatus,* less toxic organic Se forms (mainly MetSeCys, γ-Glu-MetSeCys, and a tentative selenosugar) dominate. Moreover, oxidative stress parameters (like GSH/GSSG content or SOD activity), and dose-dependent and organ-specific protein carbonylation might be responsible for diverse Se-tolerance of *Astragalus* species. The Se-induced concentration-dependent increase of H_2S levels in the sensitive *A. cicer* and its opposite change in the tolerant *A. bisulcatus* assume the participation of this reactive sulfur species in the response to Se. The results reveal connection between oxidative processes and Se sensitivitiy/tolerance/hyperaccumulation and contribute to the understanding of the molecular responses to excess Se.

CRediT authorship contribution statement

Réka Szőllősi: Investigation, Writing – original draft, Preparation, Writing – review & editing, Visualization. **Árpád Molnár:** Investigation. **Patrick Janovszky:** Investigation. **Albert Kéri:** Investigation. **Gábor Galbács:** Writing – original draft, Preparation, Writing – review & editing, Funding acquisition. **Mihály Dernovics:** Methodology, Writing – original draft, Preparation, Writing – review & editing. **Zsuzsanna Kolbert:** Conceptualization, Writing – original draft, Preparation, Writing – review & editing, Visualization, Funding acquisition.

Declaration of competing interest

The authors declare the following financial interests/personal relationships which may be considered as potential competing interests: Zsuzsanna Kolbert reports financial support was provided by National Research, Development and Innovation Office of Hungary.

Data availability

Data will be made available on request.

Acknowledgements

This work was supported by the National Research, Development and Innovation Office of Hungary under grant No. K 135303 (ZSK), K 129063 (GG) and TKP2021-NVA-19 (GG).

Authors would like to thank to Éva Kapásné Török for her valuable help during the experiments.

Appendix A. Supplementary data

Supplementary data to this article can be found online at https://doi.org/10.1016/j.plaphy.2023.107976.

References

Ağar, G., Türker, M., Battal, P., Erez, M.E., 2006. Phytohormone levels in germinating seeds of *Zea mays* L. exposed to selenium and aflatoxines. Ecotoxicology 15 (5), 443–450.

Amirabad, A.S., Behtash, F., Vafaee, Y., 2020. Selenium mitigates cadmium toxicity by preventing oxidative stress and enhancing photosynthesis and micronutrient availability on radish (*Raphanus sativus* L.) *cv*. Cherry Belle. Environ. Sci. Pollut. Res. 27 (11), 12476–12490.

Ardebili, Z.O., Ardebili, N.O., Jalili, S., Safiallah, S., 2015. The modified qualities of basil plants by selenium and/or ascorbic acid. Turk. J. Bot. 39 (3), 401–407.

Aureli, F., Ouerdane, L., Bierla, K., Szpunar, J., Prakash, N.T., Cubadda, F., 2012. Identification of selenosugars and other low-molecular weight selenium metabolites in high-selenium cereal crops. Metallomics 4 (9), 968–978.

Beers, R.F., Sizer, I.W., 1952. A spectrophotometric method for measuring the breakdown of hydrogen peroxide by catalase. J. Biol. Chem. 195 (1), 133–140.

Byrne, S.L., Durandeau, K., Nagy, I., Barth, S., 2010. Identification of ABC transporters from *Lolium perenne* L. that are regulated by toxic levels of selenium. Planta 231 (4), 901–911.

Cartes, P., Gianfreda, L., Mora, M., 2005. Uptake of selenium and its antioxidant activity in ryegrass when applied as selenate and selenite forms. Plant Soil 276, 359–367.

Chauhan, R., Awasthi, S., Srivastava, S., Dwivedi, S., Pilon-Smits, E.A., Dhankher, O.P., Tripathi, R.D., 2019. Understanding selenium metabolism in plants and its role as a beneficial element. Crit. Rev. Environ. Sci. Technol. 49 (21), 1937–1958.

Chen, Y., Mo, H.Z., Zheng, M.Y., Xian, M., Qi, Z.Q., Li, Y.Q., Hu, L.B., Chen, J., Yang, L.F., 2014. Selenium inhibits root elongation by repressing the generation of endogenous hydrogen sulfide in *Brassica rapa*. PLoS One 9 (10), e110904.

Ciacka, K., Tymiński, M., Gniazdowska, A., Krasuska, U., 2020. Carbonylation of proteins—an element of plant ageing. Planta 252 (1), 1–13.

Corpas, F.J., González-Gordo, S., Cañas, A., Palma, J.M., 2019. Nitric oxide and hydrogen sulfide in plants: which comes first? J. Exp. Bot. 70 (17), 4391–4404.

Cui, W., Chen, H., Zhu, K., Jin, Q., Xie, Y., Cui, J., Xia, Y., Zhang, J., Shen, W., 2014. Cadmium-induced hydrogen sulfide synthesis is involved in cadmium tolerance in *Medicago sativa* by reestablishment of reduced (homo) glutathione and reactive oxygen species homeostases. PLoS One 9 (10), e109669.

Das, D., Seal, P., Biswas, S., Biswas, A.K., 2020. Modulation of ascorbate-glutathione cycle by selenate and sulphate treatments in the seedlings of two rice (*Oryza sativa* L.) cultivars. Plant Sci. Today 7 (3), 441–455.

Du, B., Luo, H., He, L., Zhang, L., Liu, Y., Mo, Z., Pan, S., Tian, H., Duan, M., Tang, X., 2019. Rice seed priming with sodium selenate: effects on germination, seedling growth, and biochemical attributes. Sci. Rep. 9 (1), 1–9.

Fang, H., Jing, T., Liu, Z., Zhang, L., Jin, Z., Pei, Y., 2014. Hydrogen sulfide interacts with calcium signaling to enhance the chromium tolerance in *Setaria italica*. Cell Calcium 56 (6), 472–481.

Feng, R., Wei, C., Tu, S., Wu, F., 2009. Effects of Se on the uptake of essential elements in *Pteris vittata* L. Plant Soil 325, 123–132.

Filek, M., Zembala, M., Kornaś, A., Walas, S., Mrowiec, H., Hartikainen, H., 2010. The uptake and translocation of macro-and microelements in rape and wheat seedlings as affected by selenium supply level. Plant Soil 336 (1), 303–312.
Foyer, C.H., Noctor, G., 2011. Ascorbate and glutathione: the heart of the redox hub. Plant Physiol. 155 (1), 2–18.
Freeman, J.L., Zhang, L.H., Marcus, M.A., Fakra, S., McGrath, S.P., Pilon-Smits, E.A., 2006. Spatial imaging, speciation, and quantification of selenium in the hyperaccumulator plants *Astragalus bisulcatus* and *Stanleya pinnata*. Plant Physiol. 142 (1), 124–134.
Gouveia, G.C.C., Galindo, F.S., Lanza, M.G.D.B., da Rocha Silva, A.C., de Brito Mateus, M. P., da Silva, M.S., Tavanti, R.F.R., Tavanti, T.R., Lavres, J., Dos Reis, A.R., 2020. Selenium toxicity stress-induced phenotypical, biochemical and physiological responses in rice plants: characterization of symptoms and plant metabolic adjustment. Ecotoxicol. Environ. Saf. 202, 110916.
Grant, K., Carey, N.M., Mendoza, M., Schulze, J., Pilon, M., Pilon-Smits, E.A., Van Hoewyk, D., 2011. Adenosine 5′-phosphosulfate reductase (APR2) mutation in *Arabidopsis* implicates glutathione deficiency in selenate toxicity. Biochem. J. 438 (2), 325–335.
Griffith, O.W., 1980. Determination of glutathione and glutathione disulfide using glutathione reductase and 2-vinylpyridine. Anal. Biochem. 106 (1), 207–212.
Gupta, M., Gupta, S., 2017. An overview of selenium uptake, metabolism, and toxicity in plants. Front. Plant Sci. 7, 2074.
Halliwell, B., 2020. Reflections of an aging free radical. Free Radic. Biol. Med. 161, 234–245.
Hancock, J.T., 2019. Hydrogen sulfide and environmental stresses. Environ. Exp. Bot. 161, 50–56.
Hasanuzzaman, M., Bhuyan, M.B., Raza, A., Hawrylak-Nowak, B., Matraszek-Gawron, R., Al Mahmud, J., Nahar, K., Fujita, M., 2020. Selenium in plants: boon or bane? Environ. Exp. Bot. 178, 104170.
Hassan, A.M., Saber, N.E., Ali, A.S., El-Hosary, E.G., 2018. Interactive effect between sulfate and selenate on glutathione pool in garden rocket (*Eruca sativa* L.) leaves. J. Plant Nutr. 41 (14), 1834–1841.
Hawrylak-Nowak, B., 2013. Comparative effects of selenite and selenate on growth and selenium accumulation in lettuce plants under hydroponic conditions. Plant Growth Regul. 70 (2), 149–157.
Hawrylak-Nowak, B., Matraszek, R., Pogorzelec, M., 2015. The dual effects of two inorganic selenium forms on the growth, selected physiological parameters and macronutrients accumulation in cucumber plants. Acta Physiol. Plant. 37 (2), 1–13.
Hawrylak-Nowak, B., 2022. Biological activity of selenium in plants: physiological and biochemical mechanisms of phytotoxicity and tolerance. In: Hossain, M.A., et al. (Eds.), Selenium and Nano-Selenium in Environmental Stress Management and Crop Quality Improvement, Sustainable Plant Nutrition in a Changing World. Springer, Cham, pp. 341–363. https://doi.org/10.1007/978-3-031-07063-1_17.
Huang, D., Huo, J., Liao, W., 2021. Hydrogen sulfide: roles in plant abiotic stress response and crosstalk with other signals. Plant Sci. 302, 110733.
Khalofah, A., Migdadi, H., El-Harty, E., 2021. Antioxidant enzymatic activities and growth response of quinoa (*Chenopodium quinoa* Willd) to exogenous selenium application. Plants 10 (4), 719.
Kikkert, J., Berkelaar, E., 2013. Plant uptake and translocation of inorganic and organic forms of selenium. Arch. Environ. Contam. Toxicol. 65 (3), 458–465.
Kolbert, Zs., Pető, A., Lehotai, N., Feigl, G., Ördög, A., Erdei, L., 2012. In vivo and in vitro studies on fluorophore-specificity. Acta Biol. Szeged. 56, 37–41.
Kolbert, Z., Lehotai, N., Molnár, Á., Feigl, G., 2016. "The roots" of selenium toxicity: a new concept. Plant Signal. Behav. 11 (10), e1241935.
Kolbert, Z., Molnár, Á., Szőllősi, R., Feigl, G., Erdei, L., Ördög, A., 2018. Nitro-oxidative stress correlates with Se tolerance of *Astragalus* species. Plant Cell Physiol. 59 (9), 1827–1843.
Kolbert, Z., Molnár, Á., Feigl, G., Van Hoewyk, D., 2019a. Plant selenium toxicity: proteome in the crosshairs. J. Plant Physiol. 232, 291–300.
Kurek, E., Michalska-Kacymirow, M., Konopka, A., Kościuczuk, O., Tomiak, A., Bulska, E., 2020. Searching for low molecular weight seleno-compounds in sprouts by mass spectrometry. Molecules 25 (12), 2870.
Lapaz, A.D.M., Santos, L.F.D.M., Yoshida, C.H.P., Heinrichs, R., Campos, M., Reis, A.R.D., 2019. Physiological and toxic effects of selenium on seed germination of cowpea seedlings. Bragantia 78, 498–508.
Law, M.Y., Charles, S.A., Halliwell, B., 1983. Glutathione and ascorbic acid in spinach (*Spinacia oleracea*) chloroplasts. The effect of hydrogen peroxide and of paraquat. Biochem. J. 210 (3), 899–903.
Lehotai, N., Pető, A., Erdei, L., Kolbert, Zs., 2011. The effect of selenium (Se) on development and nitric oxide levels in *Arabidopsis thaliana* seedlings. Acta Biol. Szeged. 55 (1), 105–107.
Lehotai, N., Kolbert, Zs, Pető, A., Feigl, G., Ördög, A., Kumar, D., Tari, I., Erdei, L., 2012. Selenite-induced hormonal and signaling mechanisms during root growth of *Arabidopsis thaliana* L. J. Exp. Bot. 63, 5677–5687. https://doi.org/10.1093/jxb/ers222.
Limbeck, A., Brunnbauer, L., Lohninger, H., Pořízka, P., Modlitbová, P., Kaiser, J., Janovszky, P., Kéri, A., Galbács, G., 2021. Methodology and applications of elemental mapping by laser induced breakdown spectroscopy. Anal. Chim. Acta 1147, 72–98.
Lowry, O.H., Rosebrough, N.J., Farr, A.L., Randall, R.J., 1951. Protein measurement with the Folin phenol reagent. J. Biol. Chem. 193, 265–275.
Lv, Q., Liang, X., Nong, K., Gong, Z., Qin, T., Qin, X., Wang, D., Zhu, Y., 2021. Advances in research on the toxicological effects of selenium. Bull. Environ. Contam. Toxicol. 106 (5), 715–726.
Maassoumi, N., Ghanati, F., Zare-Maivan, H., Gavlighi, H.A., 2022. Metabolic changes network in selenium-treated *Astragalus* cells derived by glutathione as a core component. Plant Cell Tissue Organ Cult. 149 (1), 455–465.
Matamoros, M.A., Kim, A., Peñuelas, M., Ihling, C., Griesser, E., Hoffmann, R., Fedorova, M., Frolov, A., Becana, M., 2018. Protein carbonylation and glycation in legume nodules. Plant Physiol. 177 (4), 1510–1528.
Misra, H.P., Fridovich, I., 1972. The role of superoxide anion in the autoxidation of epinephrine and a simple assay for superoxide dismutase. J. Biol. Chem. 247 (10), 3170–3175.
Molnár, Á., Papp, M., Kovács, D.Z., Bélteky, P., Oláh, D., Feigl, G., Szőllősi, R., Rázga, Z., Ördög, A., Erdei, L., Rónavári, A., Kónya, Z., Kolbert, Zs., 2020. Nitro-oxidative signalling induced by chemically synthetized zinc oxide nanoparticles (ZnO NPs) in *Brassica* species. Chemosphere 251, 126419.
Ouerdane, L., Both, E.B., Xiang, J., Yin, H., Kang, Y., Shao, S., Kiszelák, K., Jókai, Z., Dernovics, M., 2020. Water soluble selenometabolome of *Cardamine violifolia*. Metallomics 12 (12), 2032–2048.
Pasricha, S., Mathur, V., Garg, A., Lenka, S., Verma, K., Agarwal, S., 2021. Molecular mechanisms underlying heavy metal uptake, translocation and tolerance in hyperaccumulators-an analysis: heavy metal tolerance in hyperaccumulators. Environ. Chall. 4, 100197 https://doi.org/10.1016/j.envc.2021.100197.
Pilon-Smits, E.A., 2019. On the ecology of selenium accumulation in plants. Plants 8 (7), 197.
Placer, Z.A., Cushman, L.L., Johnson, B.C., 1966. Estimation of product of lipid peroxidation (malonyl dialdehyde) in biochemical systems. Anal. Biochem. 16 (2), 359–364.
Ponton, D.E., Graves, S.D., Fortin, C., Janz, D., Amyot, M., Schiavon, M., 2020. Selenium interactions with algae: chemical processes at biological uptake sites, bioaccumulation, and intracellular metabolism. Plants 9 (4), 528.
Raina, M., Sharma, A., Nazir, M., Kumari, P., Rustagi, A., Hami, A., Bhau, B.S., Zargar, S. M., Kumar, D., 2020. Exploring the new dimensions of selenium research to understand the underlying mechanism of its uptake, translocation, and accumulation. Physiol. Plantarum 171 (4), 882–895.
Rajput, V.D., Singh, R.K., Verma, K.K., Sharma, L., Quiroz-Figueroa, F.R., Meena, M., Gour, V.S., Minkina, T., Sushkova, S., Mandzhieva, S., 2021. Recent developments in enzymatic antioxidant defence mechanism in plants with special reference to abiotic stress. Biology 10 (4), 267.
Ramos, S.J., Faquin, V., Guilherme, L.R.G., Castro, E.M., Ávila, F.W., Carvalho, G.S., Bastos, C.E.A., Oliveira, C., 2010. Selenium biofortification and antioxidant activity in lettuce plants fed with selenate and selenite. Plant Soil Environ. 56 (12), 584–588.
Rao, S., Yu, T., Cong, X., Lai, X., Xiang, J., Cao, J., Liao, X., Gou, Y., Chao, W., Xue, H., Cheng, S., 2021. Transcriptome, proteome, and metabolome reveal the mechanism of tolerance to selenate toxicity in *Cardamine violifolia*. J. Hazard Mater. 406, 124283.
Ribeiro, D.M., Silva Júnior, D.D., Barcellos Cardoso, F., Martins, A.O., Silva, W.A., Nascimento, W.L., Araújo, W.L., 2016. Growth inhibition by selenium is associated with changes in primary metabolism and nutrient levels in *Arabidopsis thaliana*. Plant Cell Environ 39, 2235–2246.
Ríos, J., Rosales, M.A., Blasco, B., Cervilla, L.M., Romero, L., Ruiz, J.M., 2008. Biofortification of Se and induction of the antioxidant capacity in lettuce plants. Sci. Horticult. 116, 248–255.
Schiavon, M., Pilon-Smits, E.A., 2017. The fascinating facets of plant selenium accumulation–biochemistry, physiology, evolution and ecology. New Phytol. 213 (4), 1582–1596.
Shahid, M., Niazi, N.K., Khalid, S., Murtaza, B., Bibi, I., Rashid, M.I., 2018. A critical review of selenium biogeochemical behavior in soil-plant system with an inference to human health. Environ. Pollut. 234, 915–934.
Silva, V.M., Boleta, E.H.M., Lanza, M.G.D.B., Lavres, J., Martins, J.T., Santos, E.F., dos Santos, F.L.M., Putti, F.F., Junior, E.F., White, P.J., Broadley, M.R., 2018. Physiological, biochemical, and ultrastructural characterization of selenium toxicity in cowpea plants. Environ. Exp. Bot. 150172–150182.
Soltani, E., Baskin, J.M., Baskin, C.C., Benakashani, F., 2020. A meta-analysis of the effects of treatments used to break dormancy in seeds of the megagenus *Astragalus* (Fabaceae). Seed Sci. Res. 30 (3), 224–233.
Sors, T.G., Ellis, D.R., Na, G.N., Lahner, B., Lee, S., Leustek, T., Pickering, I.J., Salt, D.E., 2005. Analysis of sulfur and selenium assimilation in *Astragalus* plants with varying capacities to accumulate selenium. Plant J. 42 (6), 785–797.
Sors, T.G., Martin, C.P., Salt, D.E., 2009. Characterization of selenocysteine methyltransferases from *Astragalus* species with contrasting selenium accumulation capacity. Plant J. 59 (1), 110–122.
Statwick, J., Majestic, B.J., Sher, A.A., 2016. Characterization and benefits of selenium uptake by an *Astragalus* hyperaccumulator and a non-accumulator. Plant Soil 404 (1), 345–359.
Szalai, G., Dernovics, M., Gondor, O.K., et al., 2022. Mutations in Rht-B1 locus may negatively affect frost tolerance in bread wheat. Int. J. Mol. Sci. 23 (14), 7969. https://doi.org/10.3390/ijms23147969.
Szőllősi, R., Molnár, A., Feigl, G., Oláh, D., Kolbert, Z., 2021. Hydrogen sulfide and nitric oxide crosstalk in plants under stress. Hydrogen Sulfide in Plant Biology: Past Present 149. https://doi.org/10.1016/B978-0-323-85862-5.00011-7.
Szőllősi, R., Molnár, Á., Oláh, D., Kondak, S., Kolbert, Z., 2022a. Selenium toxicity and tolerance in plants: recent progress and future perspectives. In: Hossain, M.A., et al. (Eds.), Selenium and Nano-Selenium in Environmental Stress Management and Crop Quality Improvement, Sustainable Plant Nutrition in a Changing World. Springer, Cham, pp. 311–324. https://doi.org/10.1007/978-3-031-07063-1_15.
Szőllősi, R., Molnár, Á., Oláh, D., Kondak, S., Kolbert, Z., 2022b. Uptake and metabolism of selenium in plants: recent progress and future perspectives. In: Hossain, M.A., et al. (Eds.), Selenium and Nano-Selenium in Environmental Stress Management and

Crop Quality Improvement, Sustainable Plant Nutrition in a Changing World. Springer, Cham, pp. 79–90. https://doi.org/10.1007/978-3-031-07063-1_5.
Tamaoki, M., Freeman, J.L., Pilon-Smits, E.A., 2008. Cooperative ethylene and jasmonic acid signaling regulates selenite resistance in *Arabidopsis*. Plant Physiol. 146 (3), 1219–1230.
Tian, M., Hui, M., Thannhauser, T.W., Pan, S., Li, L., 2017. Selenium-induced toxicity is counteracted by sulfur in broccoli (*Brassica oleracea* L. var. italica). Front. Plant Sci. 8, 1425.
Tobiasz, A., Walas, S., Filek, M., Mrowiec, H., Samsel, K., Sieprawska, A., Hartikainen, H., 2014. Effect of selenium on distribution of macro-and micro-elements to different tissues during wheat ontogeny. Biol. Plant. (Prague) 58 (2), 370–374.
Tola, A.J., Jaballi, A., Missihoun, T.D., 2021. Protein carbonylation: emerging roles in plant redox biology and future prospects. Plants (Basel) 10 (7), 1451.
Trippe III, R.C., Pilon-Smits, E.A.H., 2021. Selenium transport and metabolism in plants: phytoremediation and biofortification implications. J. Hazard Mater. 404 (B), 124178.
Van Hoewyk, D., Takahashi, H., Inoue, E., Hess, A., Tamaoki, M., Pilon-Smits, E.A., 2008. Transcriptome analyses give insights into selenium-stress responses and selenium tolerance mechanisms in *Arabidopsis*. Physiol. Plantarum 132 (2), 236–253.
Van Hoewyk, D., 2013. A tale of two toxicities: malformed selenoproteins and oxidative stress both contribute to selenium stress in plants. Ann. Bot. 112 (6), 965–972.
Valdez Barillas, J.R., Quinn, C.F., Freeman, J.L., Lindblom, S.D., Fakra, S.C., Marcus, M. A., Gilligan, T.M., Alford, É.R., Wangeline, A.L., Pilon-Smits, E.A., 2012. Selenium distribution and speciation in the hyperaccumulator *Astragalus bisulcatus* and associated ecological partners. Plant Physiol. 159 (4), 1834–1844.
Wang, Y., Böck, A., Neuhierl, B., 1999. Acquisition of selenium tolerance by a selenium non-accumulating *Astragalus* species via selection. Biofactors 9 (1), 3–10.
Wang, J., Cappa, J.J., Harris, J.P., Edger, P.P., Zhou, W., Pires, J.C., Adair, M., Unruh, S. A., Simmons, M.P., Schiavon, M., Pilon-Smits, E.A., 2018. Transcriptome-wide comparison of selenium hyperaccumulator and nonaccumulator *Stanleya* species provides new insight into key processes mediating the hyperaccumulation syndrome. Plant Biotechnol. J. 16 (9), 1582–1594.
White, P.J., 2016. Selenium accumulation by plants. Ann. Bot 117 (2), 217–235.
White, P.J., 2017. The genetics of selenium accumulation by plants. In: Pilon-Smits, E., Winkel 611, L., Lin, Z.Q. (Eds.), Selenium in Plants, Plant Ecophysiology, vol. 11. Springer, Cham, p. 612. https://doi.org/10.1007/978-3-319-56249-0_9.pp.143-163.
White, P.J., 2018. Selenium metabolism in plants. Biochim. Biophys. Acta, Gen. Subj. 1862 (11), 2333–2342.
Woch, W., Hawrylak-Nowak, B., 2019. Selected antioxidant properties of alfalfa, radish, and white mustard sprouts biofortified with selenium. Acta Agrobot. 72 (2), 1768.
Yang, H., Yang, X., Ning, Z., Kwon, S.Y., Li, M.L., Tack, F.M., Kwon, E.E., Rinklebe, J., Yin, R., 2022. The beneficial and hazardous effects of selenium on the health of the soil-plant-human system: an overview. J. Hazard Mater. 422, 126876.
Yang, L., Yang, H., Bian, Z., Lu, H., Zhang, L., Chen, J., 2022a. The defensive role of endogenous H_2S in *Brassica rapa* against mercury-selenium combined stress. Int. J. Mol. Sci. 23 (5), 2854.